JRC Scientific and Technical Reports

Bridge Design to Eurocodes
Worked examples

Worked examples presented at the Workshop "Bridge Design to Eurocodes", Vienna, 4-6 October 2010

Support to the implementation, harmonization and further development of the Eurocodes

Y. Bouassida, E. Bouchon, P. Crespo, P. Croce, L. Davaine, S. Denton, M. Feldmann, R. Frank, G. Hanswille, W. Hensen, B. Kolias, N. Malakatas, G. Mancini, M. Ortega, G. Sedlacek, G. Tsionis

Editors
A. Athanasopoulou, M. Poljansek, A. Pinto
G. Tsionis, S. Denton

EUR 25193 EN - 2012

EUROPEAN COMMISSION

The mission of the JRC is to provide customer-driven scientific and technical support for the conception, development, implementation and monitoring of EU policies. As a service of the European Commission, the JRC functions as a reference centre of science and technology for the Union. Close to the policy-making process, it serves the common interest of the Member States, while being independent of special interests, whether private or national.

European Commission
Joint Research Centre

Contact information
Address: JRC, ELSA Unit, TP 480, I-21027, Ispra (VA), Italy
E-mail: eurocodes@jrc.ec.europa.eu
Tel.: +39-0332-789989
Fax: +39-0332-789049

http://www.jrc.ec.europa.eu/

JRC 68415

EUR 25193 EN
ISBN 978-92-79-22823-0
ISSN 1831-9424
doi: 10.2788/82360

Luxembourg: Publications Office of the European Union, 2012

Printed in Italy

Acknowledgements

The work presented in this report is a deliverable within the framework of the Administrative Arrangement SI2.558935 under the Memorandum of Understanding between the Directorate-General for Enterprise and Industry of the European Commission (DG ENTR) and the Joint Research Centre (JRC) on the support to the implementation, harmonisation and further development of the Eurocodes.

Table of Contents

CHAPTER 6

Composite bridge design (EN 1994-2)

List of authors and editors

Authors

Introduction

Steve Denton, *Parsons Brinckerhoff, Chairman of CEN/TC250 Horizontal Group Bridges*

Georgios Tsionis, *University of Patras, Secretary of CEN/TC250 Horizontal Group Bridges*

Chapter 1 – Introduction to the design example

Pilar Crespo, *Ministry of Public Works (Spain)*

Laurence Davaine, *French Railway Bridge Engineering Department (SNCF, IGOA)*

Chapter 2 – Basis of design (EN 1990)

Steve Denton, *Parsons Brinckerhoff, Chairman of CEN/TC250 Horizontal Group Bridges*

Chapter 3 – Actions on bridge decks and piers (EN 1991)

Nikolaos Malakatas, *Ministry of Infrastructures, Transports and Networks (Greece)*

Pietro Croce, *Department of Civil Engineering, University of Pisa, Italy*

Chapter 4 – Bridge deck modeling and design

Laurence Davaine, *French Railway Bridge Engineering Department (SNCF, IGOA)*

Chapter 5 – Concrete bridge design (EN 1992)

Emmanuel Bouchon, *Large Bridge Division, Setra/CTOA, Paris, France*

Giuseppe Mancini, *Politecnico di Torino, Italy*

Chapter 6 – Composite bridge design (EN 1994-2)

Miguel Ortega Cornejo, *IDEAM S.A., University "Europea de Madrid', Spain*

Joel Raoul, *Large Bridge Division, Setra/CTOA, Ecole Nationale de Ponts et Chausses, Paris, France*

Chapter 7 – Geotechnical aspects of bridge design (EN 1997)

Roger Frank, *University Paris-Est, Ecole den Ponts ParisTech, Navier-CERMES*

Yosra Bouassida, *University Paris-Est, Ecole den Ponts ParisTech, Navier-CERMES*

Chapter 8 – Overview of seismic issues for bridge design (EN 1998-1, EN 1998-2)

Basil Kolias, *DENCO S.A., Athens*

Appendix A – Design of steel bridges. Overview of key content of EN 1993.

Gerhard Hanswille, *Bergische Universitat*

Wolfang Hensen, *PSP - Consulting Engineers*

Markus Feldmann, *RWTH Aachen University*
Gerhard Sedlacek, *RWTH Aachen University*

Editors

Adamantia Athanasopoulou, Martin Poljansek, Artur Pinto
European Laboratory for Structural Assessment
Institute for the Protection and Security of the Citizen
Joint Research Centre, European Commission

Georgios Tsionis, Steve Denton
CEN/TC250 Horizontal Group Bridges

Foreword

The **construction sector** is of strategic importance to the EU as it delivers the buildings and infrastructure needed by the rest of the economy and society. It represents more than **10% of EU GDP and more than 50% of fixed capital formation**. It is the largest single economic activity and the biggest industrial employer in Europe. The sector employs directly almost 20 million people. In addition, construction is a key element for the implementation of the **Single Market** and other construction relevant EU Policies, e.g.: **Environment and Energy**.

In line with the EU's strategy for smart, sustainable and inclusive growth (EU2020), **Standardization** will play an important part in supporting the strategy. The **EN Eurocodes** are a set of **European standards** which provide common rules for the design of construction works, to check their strength and stability against live and extreme loads such as earthquakes and fire.

With the publication of all the 58 Eurocodes parts in 2007, the implementation of the Eurocodes is extending to all European countries and there are firm steps towards their adoption internationally. The Commission Recommendation of 11 December 2003 stresses the importance of **training in the use of the Eurocodes**, especially in engineering schools and as part of continuous professional development courses for engineers and technicians, noting that they should be promoted both at national and international level.

In light of the Recommendation, DG JRC is collaborating with DG ENTR and CEN/TC250 "Structural Eurocodes" and is publishing the Report Series '**Support to the implementation, harmonization and further development of the Eurocodes**' as JRC Scientific and Technical Reports. This Report Series include, at present, the following types of reports:

1. Policy support documents – Resulting from the work of the JRC and cooperation with partners and stakeholders on 'Support to the implementation, promotion and further development of the Eurocodes and other standards for the building sector.
2. Technical documents – Facilitating the implementation and use of the Eurocodes and containing information and practical examples (Worked Examples) on the use of the Eurocodes and covering the design of structures or their parts (e.g. the technical reports containing the practical examples presented in the workshops on the Eurocodes with worked examples organized by the JRC).
3. Pre-normative documents – Resulting from the works of the CEN/TC250 Working Groups and containing background information and/or first draft of proposed normative parts. These documents can be then converted to CEN technical specifications.
4. Background documents – Providing approved background information on current Eurocode part. The publication of the document is at the request of the relevant CEN/TC250 Sub-Committee.
5. Scientific/Technical information documents – Containing additional, non-contradictory information on current Eurocodes parts which may facilitate implementation and use, preliminary results from pre-normative work and other studies, which may be used in future revisions and further development of the standards. The authors are various stakeholders involved in Eurocodes process and the publication of these documents is authorized by the relevant CEN/TC250 Sub-Committee or Working Group.

Editorial work for this Report Series is **assured by the JRC** together with partners and stakeholders, when appropriate. The publication of the reports type 3, 4 and 5 is made after approval for publication from the CEN/TC250 Co-ordination Group.

The publication of these reports by the JRC serves the purpose of implementation, further harmonization and development of the Eurocodes, However, it is noted that neither the Commission nor CEN are obliged to follow or endorse any recommendation or result included in these reports in the European legislation or standardization processes.

This report is part of the so-called Technical documents (Type 2 above) and contains a comprehensive description of the practical examples presented at the workshop "Bridge Design to the Eurocodes" with emphasis on worked examples of bridge design. The workshop was held on 4-6 October 2010 in Vienna, Austria and was co-organized with CEN/TC250/Horizontal Group Bridges, the Austrian Federal Ministry for Transport, Innovation and Technology and the Austrian Standards Institute, with the support of CEN and the Member States. The workshop addressed representatives of public authorities, national standardisation bodies, research institutions, academia, industry and technical associations involved in training on the Eurocodes. The main objective was to facilitate training on Eurocode Parts related to Bridge Design through the transfer of knowledge and training information from the Eurocode Bridge Parts writers (CEN/TC250 Horizontal Group Bridges) to key trainers at national level and Eurocode users.

The workshop was a unique occasion to compile a state-of-the-art training kit comprising the slide presentations and technical papers with the worked example for a bridge structure designed following the Eurocodes. The present JRC Report compiles all the technical papers prepared by the workshop lecturers resulting in the presentation of a bridge structure analyzed from the point of view of each Eurocode.

The editors and authors have sought to present useful and consistent information in this report. However, it must be noted that **the report is not a complete design example** and **that the reader may identify some discrepancies between chapters.** **Users of information contained in this report must satisfy themselves of its suitability for the purpose for which they intend to use it.** It is also noted that the chapters presented in the report have been prepared by different authors, and reflecting the different practices in the EU Member States both '**.**' and '**,**' are used as decimal separators.

We would like to gratefully acknowledge the workshop lecturers and the members of CEN/TC250 Horizontal Group Bridges for their contribution in the organization of the workshop and development of the training material comprising the slide presentations and technical papers with the worked examples. We would also like to thank the Austrian Federal Ministry for Transport, Innovation and Technology, especially Dr. Eva M. Eichinger-Vill, and the Austrian Standards Institute for their help and support in the local organization of the workshop.

All the material prepared for the workshop (slides presentations and JRC Report) is available to download from the "Eurocodes: Building the future" website (http://eurocodes.jrc.ec.europa.eu).

Ispra, November 2011

Adamantia Athanasopoulou, Martin Poljansek, Artur Pinto

European Laboratory for Structural Assessment (ELSA)

Institute for the Protection and Security of the Citizen (IPSC)

Joint Research Centre (JRC) - European Commission

Steve Denton, George Tsionis

CEN/TC250 Horizontal Group Bridges

Introduction

The Eurocodes are currently in the process of national implementation towards becoming the Europe-wide means for structural design of civil engineering works.

As part of the strategy and general programme for promotion and training on the Eurocodes, a workshop on bridge design to Eurocodes was organised in Vienna in October 2010. The main objective of this workshop was to transfer background knowledge and expertise. The workshop aimed to provide state-of-the-art training material and background information on Eurocodes, with an emphasis on practical worked examples.

This report collects together the material that was prepared and presented at the workshop by a group of experts who have been actively involved in the development of the Eurocodes. It summarises important points of the Eurocodes for the design of concrete, steel and composite road bridges, including foundations and seismic design. The worked examples utilise a common bridge project as a basis, although inevitably, they are not exhaustive.

THE EUROCODES FOR THE DESIGN OF BRIDGES

The Eurocodes

The Eurocodes, listed in the Table I, constitute a set of 10 European standards (EN) for the design of civil engineering works and construction products. They were produced by the European Committee for Standardization (CEN) and embody national experience and research output together with the expertise of international technical and scientific organisations. The Eurocodes suite covers all principal construction materials, all major fields of structural engineering and a wide range of types of structures and products.

Table I: Eurocode parts

EN 1990	Eurocode: Basis of structural design
EN 1991	Eurocode 1: Actions on structures
EN 1992	Eurocode 2: Design of concrete structures
EN 1993	Eurocode 3: Design of steel structures
EN 1994	Eurocode 4: Design of composite steel and concrete structures
EN 1995	Eurocode 5: Design of timber structures
EN 1996	Eurocode 6: Design of masonry structures
EN 1997	Eurocode 7: Geotechnical design
EN 1998	Eurocode 8: Design of structures for earthquake resistance
EN 1999	Eurocode 9: Design of aluminium structures

From March 2010, the Eurocodes were intended to be the only Standards for the design of structures in the countries of the European Union (EU) and the European Free Trade Association (EFTA). The Member States of the EU and EFTA recognise that the Eurocodes serve as:

- a means to prove compliance of buildings and civil engineering works with the essential requirements of the Construction Products Directive (Directive 89/106/EEC), particularly Essential Requirement 1 “Mechanical resistance and stability” and Essential Requirement 2 “Safety in case of fire”;
- a basis for specifying contracts for construction works and related engineering services;

- a framework for drawing up harmonised technical specifications for construction products (ENs and ETAs).

The Eurocodes were developed under the guidance and co-ordination of CEN/TC250 “Structural Eurocodes”. The role of CEN/TC250 and its subcommittees is to manage all the work for the Eurocodes and to oversee their implementation. The Horizontal Group Bridges was established within CEN/TC250 with the purpose of facilitating technical liaison on matters related to bridges and to support the wider strategy of CEN/TC250. In this context, the strategy for the Horizontal Group Bridges embraces the following work streams: maintenance and evolution of Eurocodes, development of National Annexes and harmonisation, promotion (training/guidance and international), future developments and promotion of research needs.

Bridge Parts of the Eurocodes

Each Eurocode, except EN 1990, is divided into a number of parts that cover specific aspects. The Eurocodes for concrete, steel, composite and timber structures and for seismic design comprise a Part 2 which covers explicitly the design of road and railway bridges. These parts are intended to be used for the design of new bridges, including piers, abutments, upstand walls, wing walls and flank walls etc., and their foundations. The materials covered are i) plain, reinforced and prestressed concrete made with normal and light-weight aggregates, ii) steel, iii) steel-concrete composites and iv) timber or other wood-based materials, either singly or compositely with concrete, steel or other materials. Cable-stayed and arch bridges are not fully covered. Suspension bridges, timber and masonry bridges, moveable bridges and floating bridges are excluded from the scope of Part 2 of Eurocode 8.

A bridge designer should use EN 1990 for the basis of design, together with EN 1991 for actions, EN 1992 to EN 1995 (depending on the material) for the structural design and detailing, EN 1997 for geotechnical aspects and EN 1998 for design against earthquakes. The main Eurocode parts used for the design of concrete, steel and composite bridges are given in Table II.

The ten Eurocodes are part of the broader family of European standards, which also include material, product and execution standards. The Eurocodes are intended to be used together with such normative documents and, through reference to them, adopt some of their provisions. Fig. I schematically illustrates the use of Eurocodes together with material (e.g. concrete and steel), product (e.g. bearings, barriers and parapets) and execution standards for the design and construction of a bridge.

Table II: Overview of principal Eurocode parts used for the design of concrete, steel and composite bridges and bridge elements

EN Part	Scope	Concrete	Steel	Composite
EN 1990	Basis of design	√	√	√
EN 1990/A1	Bridges	√	√	√
EN 1991-1-1	Self-weight	√	√	√
EN 1991-1-3	Snow loads	√	√	√
EN 1991-1-4	Wind actions	√	√	√
EN 1991-1-5	Thermal actions	√	√	√
EN 1991-1-6	Actions during execution	√	√	√
EN 1991-1-7	Accidental actions	√	√	√
EN 1991-2	Traffic loads	√	√	√
EN 1992-1-1	General rules	√		√
EN 1992-2	Bridges	√		√
EN 1993-1-1	General rules		√	√
EN 1993-1-5	Plated elements		√	√
EN 1993-1-7	Out-of-plane loading		√	√
EN 1993-1-8	Joints		√	√
EN 1993-1-9	Fatigue		√	√
EN 1993-1-10	Material toughness		√	√
EN 1993-1-11	Tension components		√	√
EN 1993-1-12	Transversely loaded plated structures		√	√
EN 1993-2	Bridges		√	√
EN 1993-5	Piling		√	√
EN 1994-1-1	General rules			√
EN 1994-2	Bridges			√
EN 1997-1	General rules	√	√	√
EN 1997-2	Testing	√	√	√
EN 1998-1	General rules, seismic actions	√	√	√
EN 1998-2	Bridges	√	√	√
EN 1998-5	Foundations	√	√	√

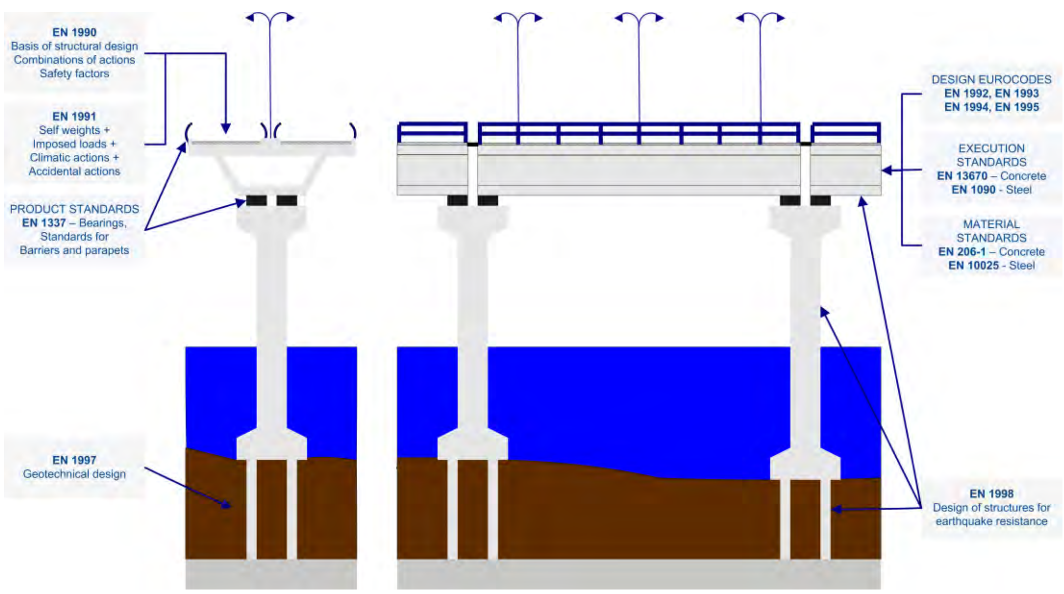

Figure I: Use of Eurocodes with product, material and execution standards for a bridge

THE DESIGN EXAMPLE

The worked examples in this report refer to the same structure. However some modifications and/or extensions are introduced to cover some specific issues that would not otherwise be addressed; details are given in the pertinent chapters. Timber bridges are not treated in this report, although their design is covered by the Eurocodes.

The following assumptions have been made:

- the bridge is not spanning a river and therefore no hydraulic actions are considered;
- the climatic conditions are such that snow actions are not considered;
- the soil properties allow for the use of shallow foundations;
- the recommended values for the Nationally Determined Parameters are used throughout.

The example structure, shown in Fig. II, is a road bridge with three spans (60.0 m + 80.0 m + 60.0 m). The continuous composite deck is made up of two steel girders with I cross-section and a concrete slab with total width 12.0 m. Alternative configurations, namely transverse connection at the bottom of the steel girders and use of external tendons, are also studied. Two solutions are considered for the piers: squat and slender piers with a height 10.0 m and 40.0 m, respectively. The squat piers have a 5.0×2.5 m rectangular cross-section while the slender piers have a circular cross-section with external diameter 4.0 m and internal diameter 3.2 m. For the case of slender piers, the deck is fixed on the piers and free to move on the abutments. For the case of squat piers, the deck is connected to each pier and abutment through triple friction pendulum isolators. The piers rest on rectangular shallow footings. The abutments are made up of gravity walls that rest on rectangular footings.

The configuration of the example bridge was chosen for the purpose of this workshop. It is not proposed as the optimum solution and it is understood that other possibilities exist. It is also noted that the example is not fully comprehensive and there are aspects that are not covered.

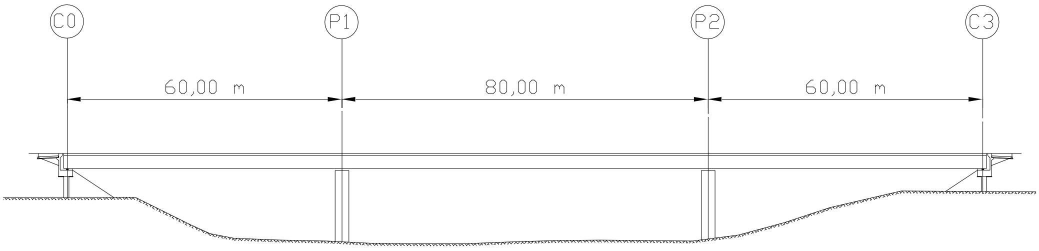

Figure II: Geometry of the example bridge

OUTLINE OF THE REPORT

Following the introduction, Chapter 1 describes the geometry and materials of the example bridge as well as the main assumptions and the detailed structural calculations. Each of the subsequent chapters presents the main principles and rules of a specific Eurocode and their application on the example bridge. The key concepts of basis of design, namely design situations, limit states, the single source principle and the combinations of actions, are discussed in Chapter 2. Chapter 3 deals with the permanent, wind, thermal, traffic and fatigue actions and their combinations. The use of FEM analysis and the design of the deck and the piers for the ULS and the SLS, including the second-order effects are presented in Chapters 4 and 5, respectively. Chapter 6 handles the classification of composite cross-sections, the ULS, SLS and fatigue verifications and the detailed design for creep and shrinkage. Chapter 7 presents the settlement and resistance calculations for the pier, three design approaches for the abutment and the verification of the foundation for the seismic design situation. Finally, Chapter 8 is concerned with the conceptual design for earthquake resistance considering the alternative solutions of slender or squat piers; the latter case involves seismic isolation and design for ductile behaviour.

Steve Denton, Chairman of Horizontal Group Bridges

Georgios Tsionis, University of Patras, Secretary of Horizontal Group Bridges

CHAPTER 6

Composite bridge design (EN1994-2)

Miguel ORTEGA CORNEJO

Project Manager. IDEAM S.A.

Prof. at University “Europea de Madrid”. Spain.

Joël RAOUL

Assistant to the Director of Large Bridge Division. Sétra/CTOA

Prof. at “Ecole Nationale de Ponts et Chaussés”. Paris. France.

Convenor EN-1994-2

6.1 Verification of cross-section at mid-span P1-P2

6.1.1 GEOMETRY AND STRESSES

At mid-span P1-P2 in ULS the concrete slab is in compression across its whole thickness. Its contribution is therefore taken into account in the cross-section resistance. The stresses in Fig. 6.1 are subsequently calculated with the composite mechanical properties and obtained by summing the various steps whilst respecting the construction phases.

The internal forces and moments in this cross-section are: M_{Ed} = 63.89 MN·m, V_{Ed} = 1.25 MN

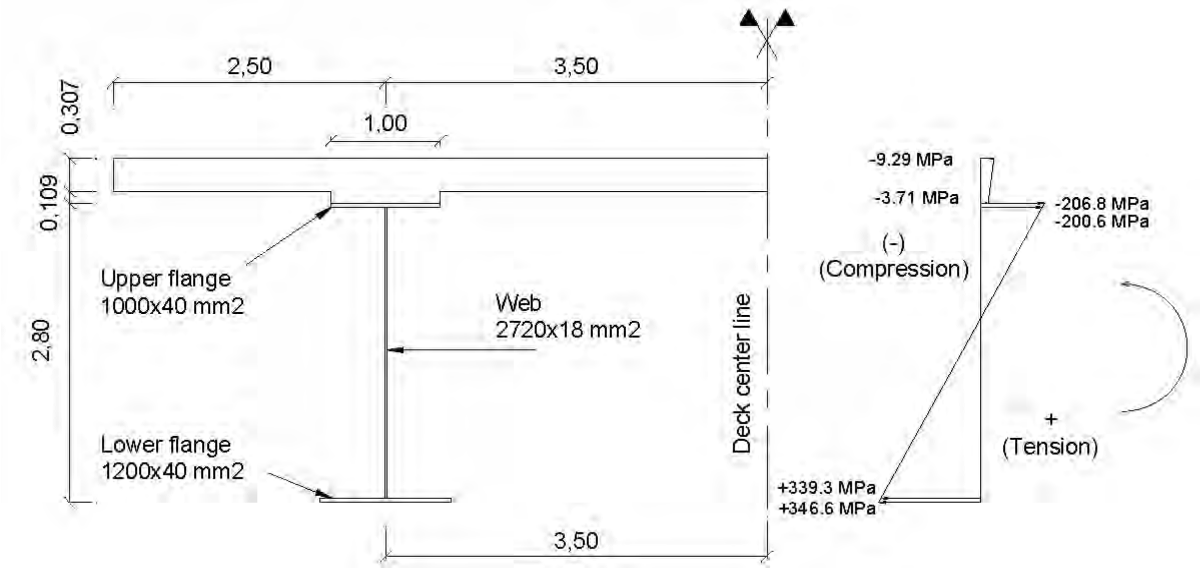

Fig. 6.1 Stresses at ULS in cross-section at mid-span P1-P2

Note: The sign criteria for stresses are according to EN-1994-2 (+) tension and (–) compression.

6.1.2 DETERMINING THE CROSS-SECTION CLASS (ACCORDING TO EN1994-2, 5.5.2)

Lower flange is in tension therefore it is Class 1. The upper flange is composite and connected following the recommendations of EN1994-2, 6.6, therefore it is Class 1.

To classify the steel web, the position of the Plastic Neutral Axis (PNA) is determined as follows:

- o Design plastic resistance of the concrete in compression:

$$F_c = A_c \frac{0.85 f_{ck}}{\gamma_c} = 1.9484 \times \frac{0.85 \cdot 35}{1.50} = 38.643\ MN \quad \text{(force of ½ slab)}$$

Note that the design compressive strength of concrete is $f_{cd} = \dfrac{f_{ck}}{\gamma_c}$ (EN-1994-2, 2.4.1.2). EN-1994 differs from EN-1992-1-1, 3.1.6 (1), in which an additional coefficient α_{cc} is applied: $f_{cd} = \dfrac{\alpha_{cc} \cdot f_{ck}}{\gamma_c}$. α_{cc} takes account of the long term effects on the compressive strength and of unfavourable effects resulting from the way the loads are applied.

The value for α_{cc} is to be given in each National annex. EN-1994-2 used the value 1.00, without permitting national choice for several reasons[1]:

- The plastic stress block for use in resistance of composite sections, defined in EN-1994, 6.2.1.2 (figure 6.2) consist of a stress *0.85f_{cd}* extending to the neutral axis, as shown in Figs. 6.2 and 6.3.

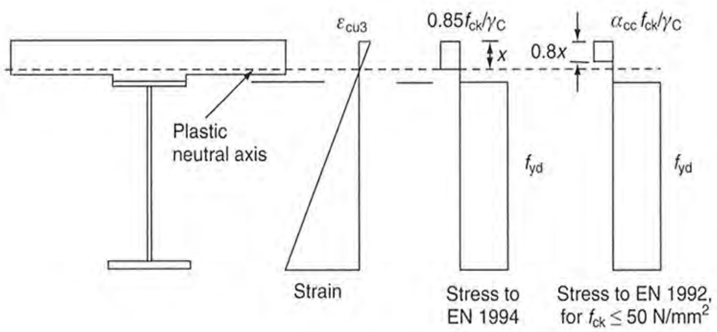

Fig. 6.2 Rectangular stress blocks for concrete in compression at ULS (figure 2.1 of[1])

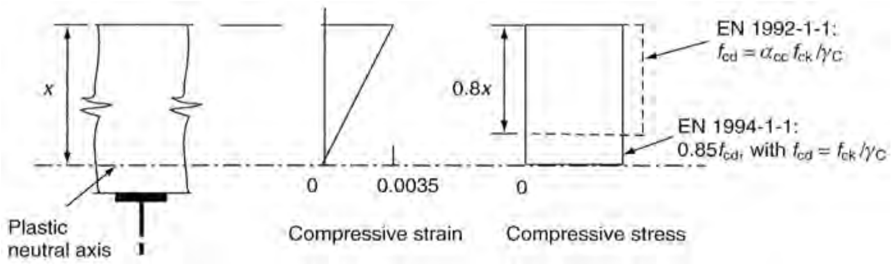

Fig 6.3 Detail of the stress block for concrete al ULS (figure 6.1 of[1])

- Predictions using the stress block of EN-1994 have been verified against the results for composite members conducted independently from the verifications for concrete bridges.
- The EN-1994 block is easier to apply. The Eurocode 2 rule for rectangular block (EN-1992-1-1, 3.1.7 (3)) was not used in Eurocode 4 because resistance formulae became complex where the neutral axis is close to or within the steel flange adjacent to concrete slab.
- Resistance formulae for composite elements given in EN-1994 are based on calibrations using stress block, with α_{cc}=1.00.

o The reinforcing steel bars in compression are neglected.

o Design plastic resistance of the structural steel upper flange (1 flange):

---

[1] See "Designers' Guide to EN-1994-2. Eurocode 4: Design of composite steel and concrete structures. Part 2: General rules and rules for bridges", C.R. Hendy and R.P. Johnson

$$F_{s,uf} = A_{s,uf}\frac{f_{y,uf}}{\gamma_{M0}} = (1.0\times0.04)\times\frac{345}{1.0} = 13.80\ MN$$

Note that for the thickness 16<t≤ 40 mm f_y=345 MPa.

- o Design plastic resistance of the structural steel web (1 web):

$$F_{s,w} = A_{s,w}\frac{f_{y,w}}{\gamma_{M0}} = (2.72\times0.018)\times\frac{345}{1.0} = 16.891\,MN$$

- o Design plastic resistance of the structural steel lower flange (1 flange):

$$F_{s,lf} = A_{s,lf}\frac{f_{y,lf}}{\gamma_{M0}} = (1.20\times0.04)\times\frac{345}{1.0} = 16.56\ MN$$

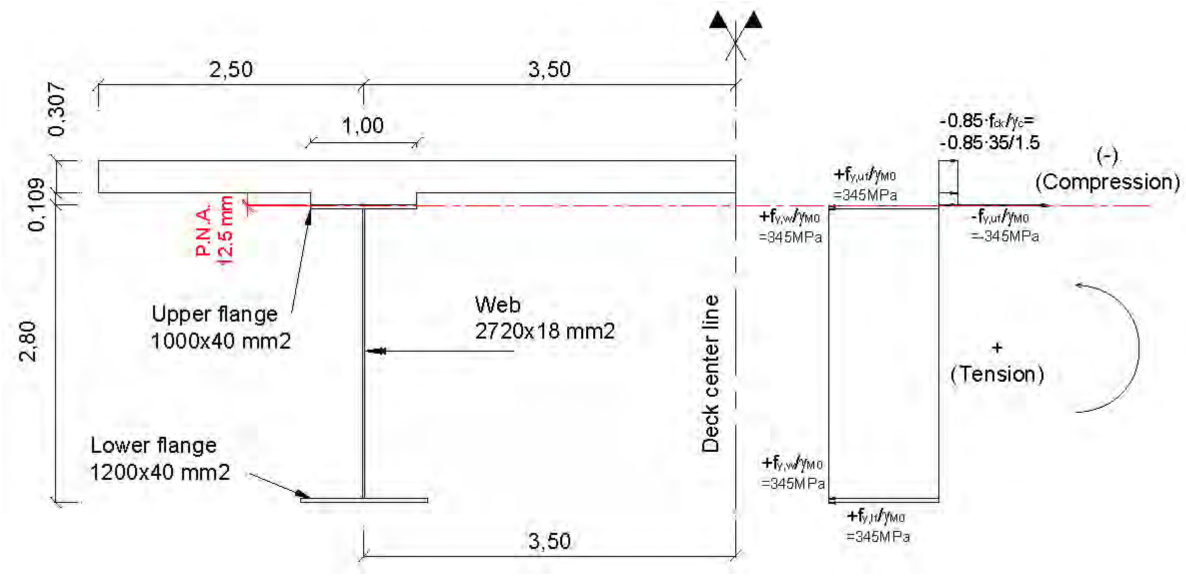

Fig. 6.4 Plastic neutral axis and design of plastic resistance moment at mid span P1-P2

As $|F_c| \le |F_{s,uf}| + |F_{s,w}| + |F_{s,lf}|$ (38.643 ≤ 47.25) and $|F_c| + |F_{s,uf}| \ge |F_{s,w}| + |F_{s,lf}|$ (52.44 ≥ 33.451) it is concluded that the PNA is located in the structural steel upper flange at a distance x from the upper extreme fibre of this flange.

The internal axial forces equilibrium of the cross section leads to the location of the PNA:

$$-F_c - F_{s,uf}\cdot x + F_{s,uf}\cdot\frac{(0.04-x)}{0.04} + F_{s,w} + F_{s,lf} = 0$$

$-38.643 - 345\cdot x + 13.8 - 345\cdot x + 16.891 + 16.56 = 0$; X=0.0125 m=12.5 mm

As the PNA is located in the upper steel flange (Fig. 6.4) the whole web and the bottom flange are in tension and therefore in Class 1 (EN-1993-1-1, 5.5.2)

Conclusion: The cross-section at mid-span P1-P2 is in Class 1 and is checked by a plastic section analysis.

This is what usually happens in composite bridges in sagging areas, with cross sections in class 1, with the PNA near or in the upper concrete slab, or at least in class 2, with only a small upper part of the compressed web.

6.1.3 PLASTIC SECTION ANALYSIS

6.1.3.1 Bending resistance check

The design plastic resistance moment is calculated from the position of the PNA according to EN1994-2, 6.2.1.2(1) (see Fig. 6.3):

$M_{pl,Rd}$ = 38.643 x (0.2505 + 0.0125) + (0.0125 x 1.0) x 345/1.0 x (0.0125/2)+ (0.0275 x 1.0) x (345/1.0) x (0.0275/2)+16.891 x (0.0275+2.72/2)+16.56 x (0.0275+2.72+0.04/2)

$M_{pl,Rd}$ = 79.59 MN·m

M_{Ed} = 63.89 MN·m ≤ $M_{pl,Rd}$ =79.59 MN·m is then verified.

The cross-section at adjacent support P1 is in Class 3 but there is no need to reduce $M_{pl,Rd}$ by a factor 0.9 because the ratio of lengths of the spans adjacent to P1 is 0.75 which is not less than 0.6 (EN1994-2, 6.2.1.3(2)).

6.1.3.2 Shear resistance check

As $\frac{h_w}{t_w} = \frac{2.72}{0.018} = 151.11 \geq \frac{31\varepsilon}{\eta}\sqrt{k_\tau} = 51.36$, the web (stiffened by the vertical stiffeners) should be checked in terms of shear buckling, according to EN-1993-1-5, 5.1.

The maximum design shear resistance is given by $V_{Rd} = min(V_{bw,Rd}\,;\,V_{pl,a,Rd})$, where $V_{bw,Rd}$ is the shear buckling resistance according to EN-1993-1-5, 5 and $V_{pl,a,Rd}$ is the resistance to vertical shear according to EN-1993-1-1, 6.2.6.

$$V_{b,Rd} = V_{bw,Rd} + V_{bf,Rd} \leq \frac{\eta f_{y,w} h_w t}{\sqrt{3}\cdot\gamma_{M1}} = \frac{1.2\times 345\times 2720\cdot 18}{\sqrt{3}\times 1.10}\times 10^{-6} = 10.63\ MN \quad \text{(EN 1993-1-5, 5.2)}$$

Given the distribution of the transverse bracing frames in the span P1-P2 (spacing a = 8 m), a vertical frame post is located in the studied cross-section (as for the cross-section at support P1). The shear buckling check is therefore performed in the adjacent web panel with the highest shear force. The maximum shear force registered in this panel is V_{Ed} = 2.21 MN.

As the vertical frame posts are assumed to be rigid:

$k_\tau = 5.34 + 4\left(\frac{h_w}{a}\right)^2 = 5.34 + 4\times\left(\frac{2.72}{8}\right)^2 = 5.802$ is the shear buckling coefficient according to EN-1993-1-5 Annex A.3

$$\sigma_E = \frac{\pi^2 \times E t_w^{\ 2}}{12\left(1-\nu^2\right)h_w^{\ 2}} = \frac{\pi^2\times 2.1\times 10^5\times 18^2}{12\times\left(1-0.3^2\right)\times 2720^2} = 8.312\ MPa \quad \text{(EN-1993-1-5 Annex A.1)}$$

$$\tau_{cr} = k_\tau \sigma_E = 5.802\times 8.312 = 48.22\ MPa \quad \text{(EN-1993-1-5, 5.3)}$$

$\bar{\lambda}_w = \sqrt{\dfrac{f_{y,w}}{\tau_{cr} \cdot \sqrt{3}}} = 0.76\sqrt{\dfrac{f_{y,w}}{\tau_{cr}}} = 0.76\sqrt{\dfrac{345}{48.22}} = 2.032$ is the slenderness of the panel according to EN-1993-1-5, 5.3. As $\bar{\lambda}_w$ is ≥1.08 then:

The factor for the contribution of the web to the shear buckling resistance χ_w is:

$$\chi_w = \frac{1.37}{\left(0.7 + \bar{\lambda}_w\right)} = \frac{1.37}{\left(0.7 + 2.032\right)} = 0.501$$ (Table 5.1. of EN-1993-1-5, 5.3)

Finally the contribution of the web to the shear buckling resistance is:

$$V_{bw,Rd} = \frac{\chi_w f_{y,w} h_w t}{\sqrt{3}\gamma_{M1}} = \frac{0.501 \times 345 \times 2720 \times 18}{\sqrt{3} \cdot 1 \times 10} \times 10^{-6} = 4.441\ MN$$

If we neglect the contribution of the flanges to the shear buckling resistance $V_{bf,Rd} \approx 0$ then:

$V_{b,Rd} = V_{bw,Rd} + V_{bf,Rd} = 4.44 + 0 \leq 10.63\ MN$; $V_{b,Rd} = 4.44\ MN$

And $V_{pl,a,Rd} = \dfrac{\eta f_{y,w} h_w t}{\sqrt{3}\gamma_{M0}} = \dfrac{1.2 \times 345 \times 2720 \times 18}{\sqrt{3} \times 1.0} E^{-6} = 11.70\ MN$ (EN 1993-1-1, 6.2.6)

So, as V_{Ed} = 2.21 MN≤ $V_{Rd} = min(V_{bw,Rd}; V_{pl,a,Rd})$= min(4.44 ; 11.70)=4.44, then is verified.

6.1.3.3 Bending and vertical shear interaction

According to EN-1994-2, 6.2.2.4 if the vertical shear force V_{Ed} does not exceed half the shear resistance V_{Rd}, obtained before, there is no need to check the interaction *M, V* (Fig. 6.5)

In our case V_{Ed} = 2.21<0.5·4.44=2.22 MN then there is no need to check the interaction M-V.

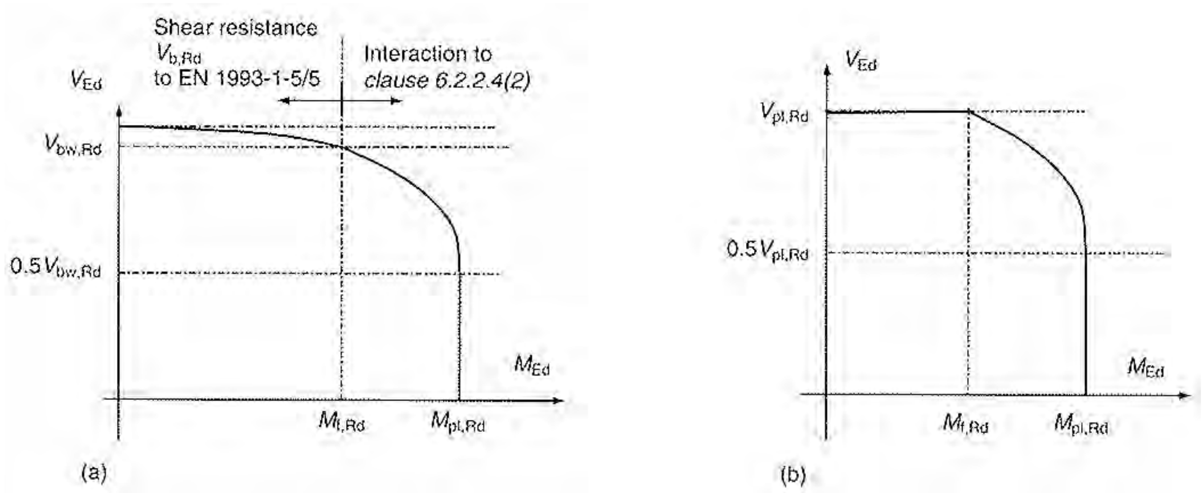

Fig. 6.5 Shear-Moment interaction for class 1 and 2 cross-sections (a) with shear buckling and without shear buckling (b). (Figure 6.6 of [1])

6.2 Verification of cross-section at internal support P1

6.2.1 GEOMETRY AND STRESSES

At internal support P1 in ULS the concrete slab is in tension across its whole thickness. Its contribution is therefore neglected in the cross-section resistance. The stresses in Fig. 6.6 are subsequently calculated and obtained by summing the various steps whilst respecting the construction phases.

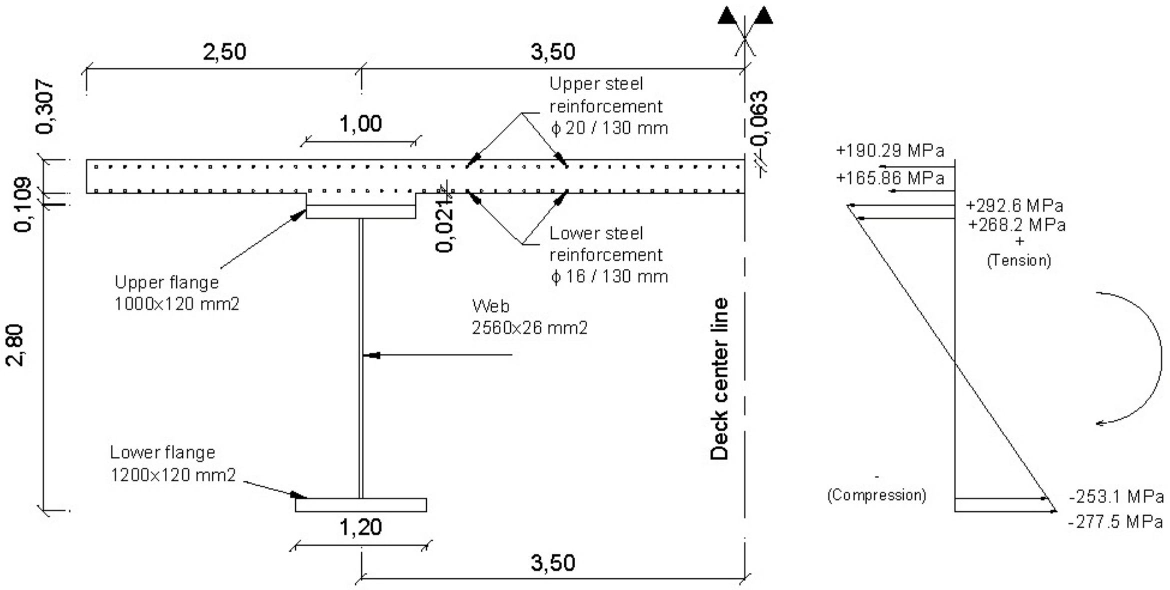

Fig. 6.6 Stresses at ULS in cross-section at internal support P1

Note: The sign criteria for stresses are according to EN-1994-2 + tension and – compression.

The internal forces and moments in this cross-section are:

M_{Ed} = -109.35 MN·m

V_{Ed} = 8.12 MN

6.2.2 DETERMINING THE CROSS-SECTION CLASS (ACCORDING TO EN1994-2, 5.5.2)

The upper flange is in tension, therefore is in Class 1 (EN 1993-1-1, 5.5.2).

The lower flange is in compression and then must be classified according to (EN 1993-1-1, Table 5.2):

$$c = \frac{b_{lf} - t_w}{2} = \frac{1200 - 26}{2} = 587\ mm$$

$$\frac{c}{t_{lf}} = \frac{587}{120} = 4.891 \leq 9\varepsilon = 9 \times \sqrt{\frac{235}{295}} = 8.033$$

(Lower flange tlf=120 mm, fy,lf=295 MPa)

Then the lower flange is in Class 1.

The web is in tension in its upper part and in compression in its lower part. The position of the Plastic Neutral Axis (PNA) is determined as follows:

- o The slab is cracked and its contribution is neglected.
- o Ultimate force of the tensioned upper reinforcing steel bars (ϕ 20/130 mm) (located in the slab):

$$F_{s,1} = A_{s,1}\frac{f_{sk}}{\gamma_s} = 144.996\times10^{-4}\,m^2\times\frac{500}{1.15} = 6.304\ MN \quad \text{(force of ½ slab)}$$

- o Ultimate force of the tensioned lower reinforcing steel bars (ϕ 16/130 mm) (located in the slab):

$$F_{s,2} = A_{s,2}\frac{f_{sk}}{\gamma_s} = 92.797\times10^{-4}\,m^2\times\frac{500}{1.15} = 4.034\ MN \quad \text{(force of ½ slab)}$$

- o Design plastic resistance of the structural steel upper flange (1 flange):

$$F_{s,uf} = A_{s,uf}\frac{f_{y.uf}}{\gamma_{M0}} = (1.2\times0.12)\times\frac{295}{1.0} = 35.4\ MN$$

- o Design plastic resistance of the total structural steel web (1 web):

$$F_{s,w} = A_{s,w}\frac{f_{y,w}}{\gamma_{M0}} = (2.56\times0.026)\times\frac{345}{1.0} = 22.963\ MN$$

- o Design plastic resistance of the structural steel lower flange (1 lower flange):

$$F_{s,lf} = A_{s.lf}\frac{f_{y,lf}}{\gamma_{M0}} = (1.20\times0.12)\times\frac{295}{1.0} = 42.48\ MN$$

As $|F_{s,1}|+|F_{s,2}|+|F_{s,uf}|\le|F_{s,w}|+|F_{s,lf}|$ (45.73≤65.44) and $|F_{s,1}|+|F_{s,2}|+|F_{s,uf}|+|F_{s,w}|\ge|F_{s,lf}|$ (68.70≤42.48) the PNA is deduced to be located in the steel web.

If we consider that the P.N.A. is located at a distance x from the upper extreme fibre of the web, then the internal axial forces equilibrium of the cross-section leads to the location of the PNA:

$$F_{s,1}+F_{s,2}+F_{s,uf}+F_{s,w}\frac{x}{2.56}-F_{s,w}\frac{(2.56-x)}{2.56}F_{s,w}-F_{s,lf}=0$$

6.304+4.034+35.4+8.97·X-22.963+8.97·X-42.48=0 ; **X=1.098 m**

Over half of the steel web is in compression (the lower part): 2.56-1.098=**1.462 m.**

$$\alpha = \frac{h_w - x}{h_w} = \frac{2.56 - 1.098}{2.56} = 0.571 > 0.50$$

Then, according to EN-1993-1-1, 5.5 and table 5.2 (sheet 1 of 3), if α>0.50 then:

The limiting slenderness between Class 2 and Class 3 is given by:

$$\frac{c}{t} = \frac{2.56}{0.026} = 98.46 >> \frac{456\varepsilon}{13\alpha - 1} = \frac{456 \cdot \sqrt{\frac{235}{345}}}{13 \cdot 0.571 - 1} = 58.59$$

The steel web is at least in Class 3 and reasoning is now based on the elastic stress distribution at ULS given in Fig. 6.6: ψ= -(268.2 / 253.1) = -1.059≤ -1 therefore the limiting slenderness between Class 3 and Class 4 is given by (EN-1993-1-1, 5.5 and table 5.2):

$$\frac{c}{t} = \frac{2.56}{0.026} = 98.46 \leq 62 \times \varepsilon \left(1 - \psi\right) \sqrt{(-\psi)} = 62 \times \sqrt{\frac{235}{345}} \times \left(1 + 1.059\right) \times \sqrt{1.059} = 108.49$$

It is concluded that the steel web is in Class 3.

Conclusion: The cross-section at support P1 is in Class 3 and is checked by an elastic section analysis.

6.2.3 SECTION ANALYSIS

6.2.3.1 Elastic bending verification

In the elastic bending verification, the maximum stresses in the structural steel must be below the yield strength $\left|\sigma_s\right| \leq \frac{f_y}{\gamma_{M0}}$.

As we have 292.63 MPa in the upper steel flange and -277.54 MPa in the lower steel flange, which are below the limit of f_y/γ_{M0}=295MPa admitted in an elastic analysis for the thickness of 120 mm, the bending resistance is verified.

This verification could be made, not with the extreme fibre stresses, but with the stresses of the center of gravity of the flanges (EN-1993-1-1, 6.2.1(9)).

6.2.3.2 Alternative: Plastic bending verification (Effective Class 2 cross-section)

EN-1994-2, 5.5.2(3) establishes that a cross-section with webs in Class 3 and flanges in Classes 1 or 2 may be treated as an effective cross-section in Class 2 with an effective web in accordance to EN-1993-1-1, 6.2.2.4.

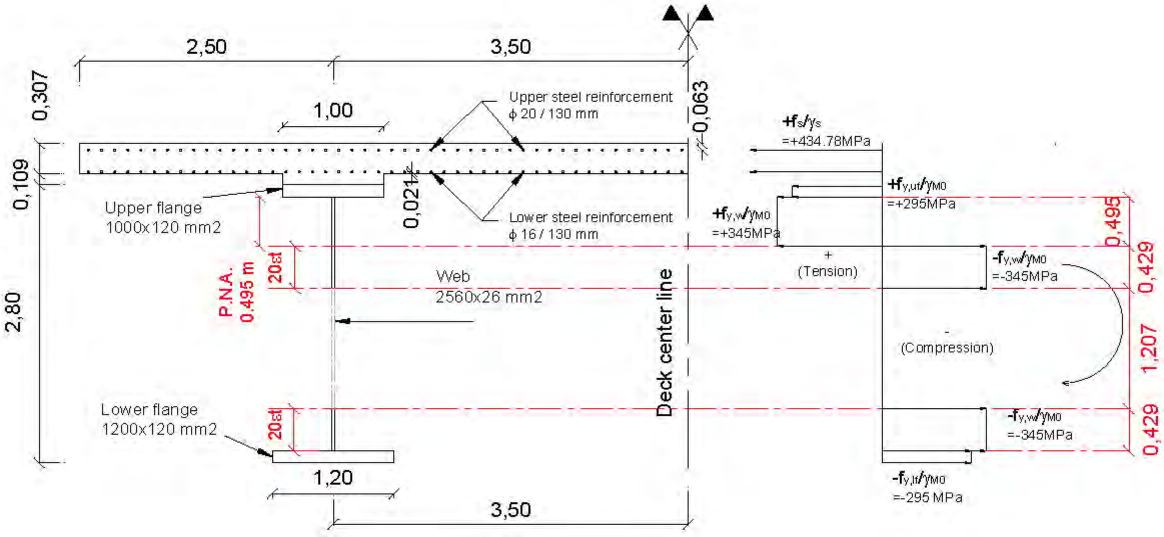

Fig. 6.7 Effective class 2 cross-section at support P-1. Design plastic bending resistance

If we consider that the PNA is located at a distance x from the extreme upper fibre of the upper part of the web, then the internal axial forces equilibrium of the cross section leads to the location of the PNA:

$$F_{s,1} + F_{s,2} + F_{s,uf} + X \times t_w \frac{f_{y,w}}{\gamma_{M0}} - 2 \times \left(20 \times \varepsilon \times t_w \times \frac{f_{y,w}}{\gamma_{M0}} \right) - F_{s,lf} = 0$$

6.304+4.034+35.4+8.97·X-2·3.848-42.48=0 , then **X=0.495 m**

And the hogging bending moment resistance of the effective class 2 cross-section is:

***M*$_{pl,Rd}$**=-(6.304·(0.353+0.12+0.495)+4.034·(0.13+0.12+0.495)+35.4·(0.06+0.495)+4.44·(0.495/2) +3.848·(2.56-0.495-0.429/2)+42.48·(2.56-0.495-0.06))= **-122.97 MN·m**

As $\left|M_{Ed}\right| = 109.35 < \left|M_{pl,Rd}\right| = 122.53$ the bending resistance is verified.

6.2.3.3 Shear resistance check

As $\frac{h_w}{t_w} = \frac{2.56}{0.026} = 98.46 \geq \frac{31\varepsilon}{\eta}\sqrt{k_\tau} = 51.36$, the web (stiffened by the vertical stiffeners) should be checked in terms of shear buckling, according to EN-1993-1-5, 5.1.

The maximum design shear resistance is given by $V_{Rd} = min(V_{bw,Rd}\,;\,V_{pl,a,Rd})$, where $V_{bw,Rd}$ is the shear buckling resistance according to EN-1993-1-5, 5 and $V_{pl,a,Rd}$ is the resistance to vertical shear according to EN-1993-1-1, 6.2.6.

$$V_{b,Rd} = V_{bw,Rd} + V_{bf,Rd} \leq \frac{\eta f_{y,w} h_w t}{\sqrt{3}\gamma_{M1}} = \frac{1.2 \times 345 \times 2560 \times 26}{\sqrt{3} \cdot 1 \times 10} \times 10^{-6} = 14.46\ MN \quad \text{(EN 1993-1-5, 5.2)}$$

Given the distribution of the bracing transverse frames (spacing a = 8 m), a vertical frame post is located in the cross-section at support P1. The shear buckling check is therefore performed in the adjacent web panel with the highest shear force. The maximum shear force registered in this panel is V_{Ed} = 8.12 MN.

The vertical frame posts are assumed to be rigid. This yields:

$k_\tau = 5.34 + 4\left(\frac{h_w}{a}\right)^2 = 5.34 + 4\left(\frac{2.56}{8}\right)^2 = 5.75$ is the shear buckling coefficient according to EN-1993-1-5 Annex A.3

$$\sigma_E = \frac{\pi^2 E t_w^{\ 2}}{12\left(1-\nu^2\right) h_w^{\ 2}} = \frac{\pi^2 \times 2.1\times 10^5 \times 26^2}{12\times\left(1-0.3^2\right)\times 2560^2} = 19.58\ MPa \text{ (EN-1993-1-5 Annex A.1)}$$

$$\tau_{cr} = k_\tau \cdot \sigma_E = 5.75\times 19.58 = 112.58\ MPa \text{ (EN-1993-1-5, 5.3)}$$

$\bar{\lambda}_w = \sqrt{\frac{f_{y,w}}{\tau_{cr}\cdot\sqrt{3}}} = 0.76\sqrt{\frac{f_{y,w}}{\tau_{cr}}} = 0.76\sqrt{\frac{345}{112.58}} = 1.33$ is the slenderness of the panel according to EN-1993-1-5, 5.3. As $\bar{\lambda}_w$ is ≥1.08 then:

The factor for the contribution of the web to the shear buckling resistance χ_w is:

$$\chi_w = \frac{1.37}{\left(0.7+\bar{\lambda}_w\right)} = \frac{1.37}{\left(0.7+1.33\right)} = 0.675 \text{ (Table 5.1. of EN-1993-1-5, 5.3)}$$

Finally the contribution of the web to the shear buckling resistance is:

$$V_{bw,Rd} = \frac{\chi_w f_{y,w} h_w t}{\sqrt{3}\gamma_{M1}} = \frac{0.675\times 345\times 2560\times 26}{\sqrt{3}\times 1.10}\times 10^{-6} = 8.14\ MN$$

If we neglect the contribution of the flanges to the shear buckling resistance $V_{bf,Rd} \approx 0$ then:

$$V_{b,Rd} = V_{bw,Rd} + V_{bf,Rd} = 8.14 + 0 \leq 14.46\ MN\ ;\ V_{b,Rd} = 8.14\ MN$$

And $V_{pl,a,Rd} = \frac{\eta f_{y,w} h_w t}{\sqrt{3}\gamma_{M0}} = \frac{1.2\times 345\times 2560\times 26}{\sqrt{3}\times 1.0}\times 10^{-6} = 15.91\ MN$ (EN 1993-1-1, 6.2.6)

As V_{Ed} = 8.12 MN≤ $V_{Rd} = min(V_{bw,Rd}\ ;\ V_{pl,a,Rd})$= min(8.14 ; 15.91)=8.14, the shear design force is lower than the shear buckling resistance.

6.2.3.4 Flange contribution to the shear buckling resistance

When the flange resistance is not fully used to resist the design bending moment, and therefore M_{Ed}<$M_{f,Rd}$ the contribution from the flanges could be evaluated according to EN-1993-1-5, 5.4.

$$V_{bf,Rd} = \frac{b_f t_f^{\ 2} f_{yf}}{c\gamma_{M1}}\left(1-\left(\frac{M_{Ed}}{M_{f,Rd}}\right)^2\right)$$

Note that in our case it is not strictly necessary the use of the shear buckling resistance of the flanges, as seen in the previous paragraph, but we will develop the calculation in an academic way.

Where b_f, and t_f must be taken for the flange which provides the smallest axial resistance, with the condition that b_f must be not larger than $15\varepsilon t_f$ on each side of the web.

$M_{f,Rd}$ is the plastic bending resistance of the cross-section neglecting the web area.

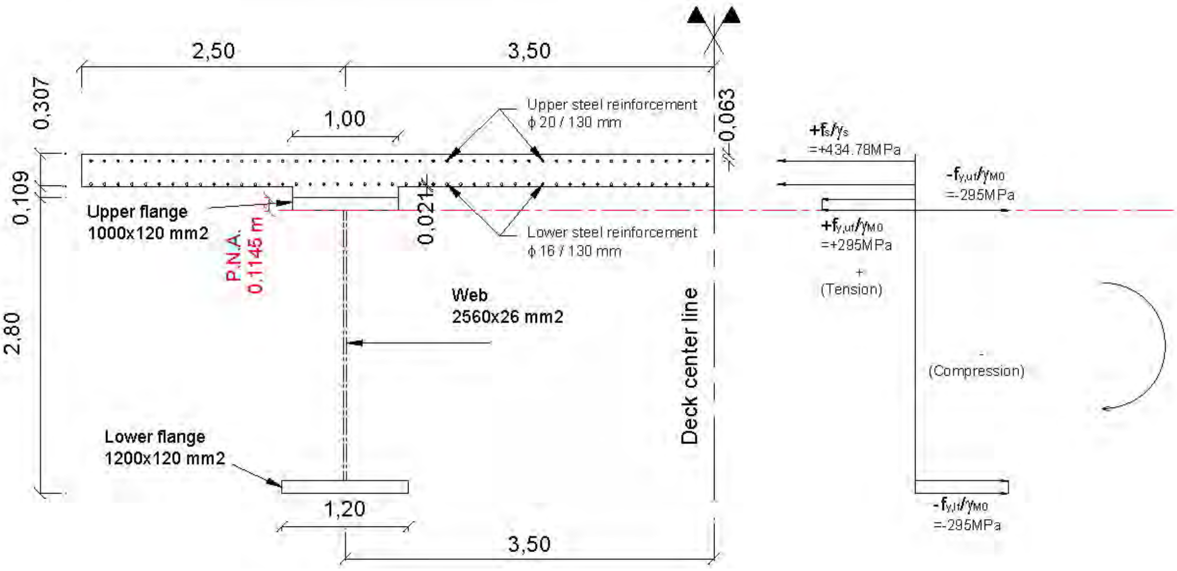

Fig. 6.8 Design plastic bending resistance neglecting the web area

If we consider that the PNA is located at a distance x from the extreme upper fibre of the upper flange, then the internal axial forces equilibrium of the cross section leads to the location of the PNA:

$$F_{s,1} + F_{s,2} + F_{s,uf}\frac{x}{0.12} - F_{s,uf}\frac{(0.12 - x)}{0.12} - F_{s,lf} = 0$$

$$6.304 + 4.034 + 35.4 \cdot \frac{x}{0.12} - 35.4 \cdot \frac{(0.12 - x)}{0.12} - 42.48 = 0$$

Then x =0.1145 m

And the hogging bending moment resistance of the effective cross-section neglecting the web area is:

Mf,Rd=-2·(6.304·(0.353+0.1145)+4.034·(0.13+0.1145)+33.777·(0.1145/2)+1.628·(0.12-0.1145)/2+42.48·(2.8-0.06-0.1145))= -117.40 MN·m.

As $|M_{Ed}| = 109.35 < |M_{f,Rd}| = 117.40$, the bending resistance is verified without considering the influence of the web, and the shear resistance is already verified neglecting the contribution of the flanges, there's no need no verify the interaction M-V. However we will check the interaction M-V for the example.

Once the bending resistance of the cross-section neglecting the web Mf,Rd is obtained, the contribution of the flanges to the shear buckling resistance can be evaluated as:

$$V_{bf,Rd} = \frac{b_f t_f^{\,2} f_{yf}}{c \cdot \gamma_{M1}}\left(1 - \left(\frac{M_{Ed}}{M_{f,Rd}}\right)^2\right)$$

As the upper flange is a composite flange, made of the steel reinforcement and the steel upper flange itself, we will take the lower steel flange (1200x120 mm2) to evaluate the contribution of the flanges to the shear buckling resistance

According to EN-1993-1-5, 5.4 (1):

$$c = a\left(0.25 + \frac{1.6 b_f t_f^{\,2} f_{yf}}{t h_w^{\,2} f_{yw}}\right) = 8\left(0.25 + \frac{1.6 \times 1200 \times 120^2 \times 295}{26 \times 2.56^2 \times 345}\right) = 3.110\ m$$

Then: $V_{bf,Rd} = \dfrac{1200 \times 120^2 \times 295}{3110 \times 1.1} \cdot \left(1 - \left(\dfrac{109.35}{117.40}\right)^2\right) 10^{-6} = 0.197 \text{ MN}$

The shear buckling resistance is the sum of the contribution of the web, $V_{bw,Rd} = 8.14\ MN$, obtained before, and the contribution of the flanges $V_{bf,Rd} = 0.197$ MN, so the total shear buckling resistance in this case is

$$V_{b,Rd} = V_{bw,Rd} + V_{bf,Rd} = 8.14 + 0.197 \leq 14.46\ MN\ ;\ V_{b,Rd} = 8.337\ MN$$

The contribution of the flanges to shear buckling resistance represents in this case less than 2.5%, which could be considered negligible as supposed before.

According to EN-1993-1-5, 5.5, the shear verification is:

$\eta_3 = \dfrac{V_{Ed}}{V_{b,Rd}} \leq 1.0$; and in this case $\eta_3 = \dfrac{8.12}{8.14} = 0.9975$ without considering the contribution of the flanges to the shear buckling resistance.

6.2.3.5 Bending and shear interaction

The interaction *M-V* should be considered according to EN-1993-1-5, 7.1 (1). As the design shear force is higher than 50% of the shear buckling resistance then is has to be verified:

$$\bar{\eta}_1 + \left[1 - \frac{M_{f,Rd}}{M_{pl,Rd}}\right]\left[2\bar{\eta}_3 - 1\right]^2 \leq 1.0$$

Where:

$$\bar{\eta}_1 = \frac{M_{Ed}}{M_{pl,Rd}},\ \text{and}\ \bar{\eta}_3 = \frac{V_{Ed}}{V_{bw,Rd}}$$

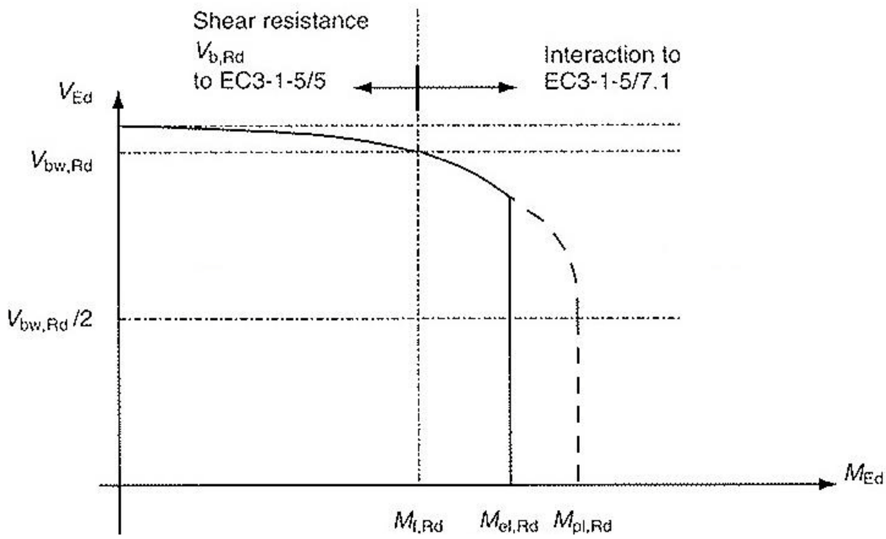

Fig. 6.9 Shear-Moment interaction for Class 3 and 4 cross-sections according to clause 7.1 of EN-1993-1-5. (Figure 6.7 of[1])

This criterion should be verified, according to EN-1993-1-5. 7.1 (2) at all sections other than those located at a distance less than $h_w/2$ from a support with vertical stiffener.

If we consider the internal shear forces and moments of the section located over P-1 (x=60m):V_{Ed}=8.124MN, M_{Ed}=-109.35mMN, and the section located at X=62.5 m: V_{Ed}=7.646MN, M_{Ed}=-91.86mMN, we could obtain the values of the design shear force and bending moment of the section located at X=61.25 m, which approximately is at $h_w/2$ from the support, as an average of both values, on the safe side:

Then, we will verify the interaction for the design internal forces and moments:

V_{Ed}=(8.124+7.646)/2=7.885 MN, and M_{Ed}=(-109.35-91.86)/2=-100.605 mMN

That leads to: $\bar{\eta}_1 = \dfrac{100.605}{122.97} = 0.818$; $\bar{\eta}_3 = \dfrac{7.885}{8.14} = 0.9686$, and:

$$\bar{\eta}_1 + \left[1 - \frac{M_{f,Rd}}{M_{pl,Rd}}\right]\left[2\bar{\eta}_3 - 1\right]^2 = 0.818 + \left[1 - \frac{117.40}{122.97}\right]\left[2 \times 0.9686 - 1\right]^2 = 0.858 \leq 1$$

So the interaction *M-V* is verified.

Note that we have considered that Mpl,Rd is the value obtained before for the effective class 2 cross-section.

6.3 Alternative double composite cross-section at internal support P-1

As an alternative to the simple composite cross-section located at the hogging bending moments area, it is possible to design a double composite cross-section, with a bottom concrete slab located between the two steel girders, connected to them.

The double composite action in hogging areas is an economical alternative to reduce the steel weight of the compressed bottom flange.

Compression stresses from negative bending usually keep the bottom slab uncracked, so bending and torsional stiffness in these areas are noticeably higher than those classically obtained with steel sections. Double composite action greatly improves the deformational and dynamic response both to bending and torsion.

The main structural advantage of the double composite action is related to the bridge response at ultimate limit state. Cross-sections along the whole bridge are in Class 1 or Class 2, not only in sagging areas, but also usually in hogging areas. Thus instability problems at ultimate limit state are avoided: not only at the bottom flange because of its connection to the concrete, but also in webs, due to the low position of the neutral axis in an ultimate limit state.

As a result, a safe and economical design is possible using a global elastic analysis with cross-section elastoplastic resistances, both in sagging and hogging areas. There is even enough capacity for almost reaching global plasticity in ULS by means of adequate control of elastoplastic rotations with no risk of brittle instabilities. This constitutes a structural advantage of the cross sections with double composite action solution when compared to the more classical twin girder alternatives.

Fig. 6,10 shows two examples of road bridges, bridge over river Mijares (main span 64 m) in Betxi-Borriol (Castellón, Spain), and bridge over river Jarama (main span 75 m) in Madrid, Spain, with double composite action in hogging areas.

Fig. 6.10 Two examples of road composite bridges with double composite action in hogging areas

Fig. 6.11 shows a view of Viaduct “Arroyo las Piedras” in the Spanish High Speed Railway Line Córdoba-Málaga. This is the first composite steel-concrete Viaduct of the Spanish railway lines, with a main span of 63.5 m.

In High Speed bridges the typical twin girder solution for road bridges must improve their torsional stiffness in order to respond to the high speed railway requirements. In this case, in hogging areas the double composite action is materialized not only for bending but also for torsion.

The double composite action was extended to the whole length of the deck to allow the torsion circuit to be closed. A strict box cross section is obtained in sagging areas with the use of discontinuous precast slabs only connected to the steel girders for torsion and not for bending.

Fig. 6.11 Example of a High Speed Railway Viaduct with double composite action

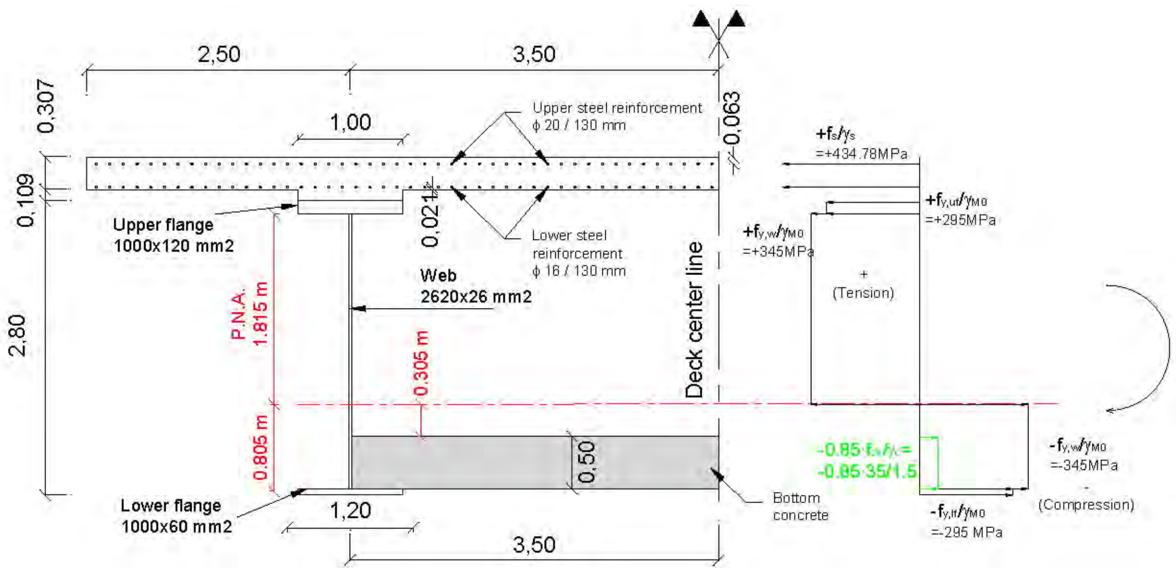

Fig. 6.12 Cross-section at support P-1 with double composite action. Design plastic bending resistance

Back to our case study, if we change the lower steel flange from 1200x120 mm^2 to a smaller one, of 1000x60 mm^2 plus a 0.50 m thick bottom slab of concrete C35/45 (Fig. 6.12), we could verify the bending resistance to compare both cross sections. We could also resize the upper steel flange or even the upper slab reinforcement, but for this example, we will keep the original ones and only change the lower steel flange.

Fig. 6.13 shows a classical solution for composite road bridges with double composite action. The bottom concrete slab, in hogging areas, is extended to a length of 20 or 25% of the main span. The maximum thickness at support cross section is 0.50 m and the minimum thickness at the end of the slab is 0.25 m. Fig. 6.13 defines in red line the thickness distribution of the bottom concrete slab, and in green the lower steel flange reduction.

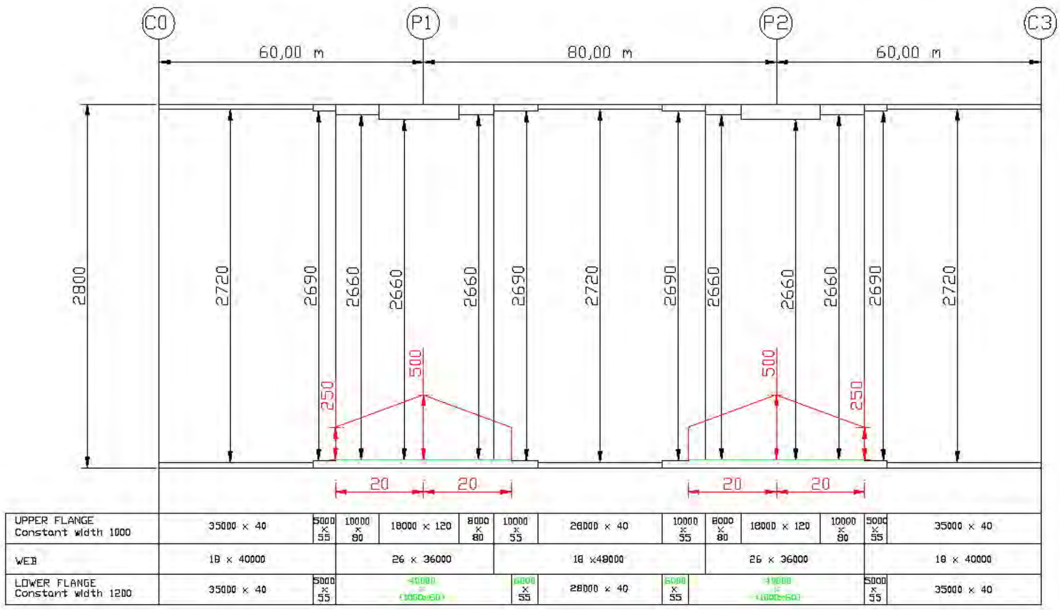

Fig. 6.13 Alternative steel distribution of the double composite main girder and bottom concrete slab thickness

For the example we are only calculating the ultimate bending resistance of the double composite cross section at support P-1, but it is necessary to clarify some aspects treated by EN-1994-2 related to the double composite action.

EN 1994-2, establishes in 5.4.2.2 (2) the modular ratio simplified method for considering the creep and shrinkage of concrete in a simple composite cross-section. For double composite cross sections this simplified method is not fully applicable.

EN-1994-2, 5.4.2.2 (10) requires that for double composite cross section with both slabs un-cracked (e.g. in the case of pre-stressing) the effects of creep and shrinkage should be determined by more accurate methods.

Strictly speaking, in our case, we do not have double composite action with both slabs un-cracked, because the upper slab will be cracked, and we will neglect its contribution and only consider the upper reinforcement, so what we have in hogging areas is a simple composite cross-section with the reinforcement of the upper slab and bottom concrete in compression.

6.3.1 DETERMINING THE CROSS-SECTION CLASS (ACCORDING TO EN1994-2, 5.5.2)

The upper flange is in tension therefore it is in Class 1 (EN 1993-1-1, 5.5.2).

The lower flange is in compression, and then must be classified according to (EN 1993-1-1, Table 5.2):

$$c = \frac{b_{lf} - t_w}{2} = \frac{1000 - 26}{2} = 487 \text{ mm}$$

$$\frac{c}{t_{lf}} = \frac{487}{60} = 8.116 \leq 10{\cdot}\varepsilon = 10{\cdot}\sqrt{\frac{235}{335}} = 8.375$$

(Lower flange t_{lf}=60 mm, $f_{y,lf}$=335 MPa)

Then the lower flange is in Class 2.

The upper part of the web is in tension and the lower part is in compression. The position of the Plastic Neutral Axis (PNA) is determined as follows:

- The tensioned upper slab is cracked and we neglect its contribution.
- Ultimate force of the tensioned upper reinforcing steel bars (ϕ 20/130 mm) (located in the slab):

$$F_{s,1} = A_{s,1}\frac{f_{sk}}{\gamma_s} = 144.996\times10^{-4}\, m^2 \times \frac{500}{1.15} = 6.304 \text{ MN} \quad \text{(force of ½ slab)}$$

- Ultimate force of the tensioned lower reinforcing steel bars (ϕ 16/130 mm) (located in the slab):

$$F_{s,2} = A_{s,2}\frac{f_{sk}}{\gamma_s} = 92.797\times10^{-4}\, m^2 \times \frac{500}{1.15} = 4.034 \text{ MN} \quad \text{(force of ½ slab)}$$

- Design plastic resistance of the structural steel upper flange (1 flange):

$$F_{s,uf} = A_{s,uf}\frac{f_{y.uf}}{\gamma_{M0}} = (1.2\times0.12)\times\frac{295}{1.0} = 35.4 \text{ MN}$$

- Design plastic resistance of the total structural steel web (1 web):

$$F_{s,w} = A_{s,w}\frac{f_{y,w}}{\gamma_{M0}} = (2.62\times 0.026)\times\frac{345}{1.0} = 23.50 \text{ MN}$$

- Design plastic resistance of the structural steel lower flange (1 lower flange):

$$F_{s,lf} = A_{s.lf}\frac{f_{y,lf}}{\gamma_{M0}} = (1.00\times 0.06)\times\frac{335}{1.0} = 20.1 \text{ MN}$$

- Design plastic resistance of the bottom concrete slab in compression:

$$F_{c,\inf} = A_c\frac{0.85 f_{ck}}{\gamma_c} = 3.5\times 0.5\times\frac{0.85\times 35}{1.50} = 34.7 \text{ MN}$$

As $\left|F_{s,1}\right| + \left|F_{s,2}\right| + \left|F_{s,uf}\right| \le \left|F_{s,w}\right| + \left|F_{s,lf}\right| + \left|F_{c,\inf}\right|$ (45.73≤78.3) and $\left|F_{s,1}\right| + \left|F_{s,2}\right| + \left|F_{s,uf}\right| + \left|F_{s,w}\right| \ge \left|F_{s,lf}\right| + \left|F_{c,\inf}\right|$ (69.23≤54.8) the PNA is located in the steel web.

If we consider that the P.N.A. is located at a distance x from the upper extreme fibre of the web, then the internal axial forces equilibrium of the cross-section gives the location of the PNA:

$$F_{s,1} + F_{s,2} + F_{s,uf} + F_{s,w}\frac{x}{2.62} - F_{s,w}\frac{(2.62-x)}{2.62}F_{s,w} - F_{s,lf} - F_{c,\inf} = 0$$

6.304+4.034+35.4+8.97·X-23.5+8.97·X-54.8=0; **X=1.815 m**

Only around 30% of the steel web is in compression (the lower part): 2.62-1.815=**0.805 m.**

$$\alpha = \frac{h_w - x}{h_w} = \frac{2.62-1.815}{2.62} = 0.307 \le 0.50$$

Then according to EN-1993-1-1, 5.5 and table 5.2 (sheet 1 of 3), if α<0.50 then:

Therefore the limiting slenderness between Class 2 and Class 3 is given by:

$$\frac{c}{t} = \frac{2.62}{0.026} = 100.76 < \frac{41.5\varepsilon}{\alpha} = \frac{41.5\times\sqrt{\frac{235}{345}}}{0.307} = 111.56$$

According to this, the steel web is in Class 2.

However, the part of the web in touch with the bottom concrete slab, is laterally connected to it, so only 0.305 m of the total length under compression (0.805 m) could have buckling problems. If we take this into consideration, the actual depth of the web considered for the classification of the compressed panel, is 1.815+0.305=2.12m instead of 2.62 m, considered before.

With this new values, $\alpha = \frac{h^*_w - x}{h^*_w} = \frac{2.12-1.815}{2.12} = 0.144 \le 0.50$

Then according to EN-1993-1-1, 5.5 and table 5.2 (sheet 1 of 3), if α<0.50 then:

Therefore the limiting slenderness between Class 1 and Class 2 is given by:

$$\frac{c}{t} = \frac{2.12}{0.026} = 81.54 < \frac{36\varepsilon}{\alpha} = \frac{36 \times \sqrt{\frac{235}{345}}}{0.144} = 206.33$$

The steel web could be in fact classified as Class 1.

Conclusion: The cross-section at support P1 with double composite action is in Class 2 (due to the lower steel flange), and can be checked by plastic section analysis, as we said at the beginning of this section.

6.3.2 PLASTIC SECTION ANALYSIS. BENDING RESISTANCE CHECK

If we consider that the PNA is located at a distance x=1.815 m from the upper extreme fibre of the upper part of the web, then the hogging bending moment resistance of the Class 2 cross-section is:

$\boldsymbol{M_{pl,Rd}}$=-(6.304·(0.353+0.12+1.815)+4.034·(0.13+0.12+1.815)+35.4·(0.06+1.815)+ 16.28·(1.185/2) +7.22·(0.805/2)+34.72·(0.805-0.25)+20.1·(0.805+0.06/2))= **-142.85 MN·m**

In comparison with the simple composite action cross-section we have significantly increased the bending moment resistance, locally reducing the amount of structural steel just by adding the bottom concrete slab connected to the steel girders.

For the final verification M_{Ed} should be lower than the ultimate bending resistance $M_{pl,Rd}$. For the example we haven't recalculated the new design bending moment M_{Ed}, increased by the self weight of the bottom concrete, something that of course should had been done in a real case.

6.3.3 SOME COMMENTS ABOUT AN EVENTUAL CRUSHING OF THE EXTREME FIBRE OF THE BOTTOM CONCRETE

EN-1994-2, 6.2.1.2 (2) establishes that for a composite cross-section with structural steel grade S420 or S460, if the distance between the PNA (x_{pl}) and the extreme fiber of the concrete slab in compression exceeds 15% of the overall depth of the cross section (h), the design resistance moment M_{Rd} should be taken as $\beta \cdot M_{Rd}$, reduced by the β factor defined on figure 6.3 of EN-1994-2. This figure limits this ratio to a maximum value of 40%.

Although this paragraph applies to the steel grade, we could consider limiting the maximum ratio x_{pl}/h to avoid an eventual crushing of the concrete.

In standard composite bridges, in sagging bending moment areas, the ratio x_{pl}/h is usually below the limit of 0.15. This value generally varies from 0.10 to 0.15, so there is not a practical incidence of the reduction of the bending moment resistance.

Meanwhile in composite cross-sections with double composite action, in hogging bending moment areas, the ratio x_{pl}/h is usually around 25-30%. The incidence of the β factor, in a real case of double composite action, has not a very big influence, barely reducing the plastic bending moment resistance of the composite cross-section from 94 to 91% of its total plastic bending resistance.

In our case study, for the alternative double composite cross-section, this ratio is x_{pl}/h=0.865/3.216=0.269. This value leads to a β factor of 0.93, so the reduced bending moment resistance would be $\beta \cdot M_{Rd}$ =0.93·(-142.85)=**-132.85 MN·m.**

In our case study we have considered the resistance of the bottom concrete, equal to the upper concrete C35/45, but in practice it is not unusual to use higher resistance in the bottom concrete: C40/50, C45/55, or even C50/60.

6.4 Verification of the Serviceability Limit States (SLS)

EN-1994-2, 7.1 (1) establishes that a composite bridge shall be designed such that all the relevant SLS are satisfied according to the principles of EN-1990, 3.4. The limit states that concern are:

- The functioning of the structure or structural members under normal use.
- The comfort of people.
- The “appearance” of the construction work. This is related with such criteria as high deflections and extensive cracking, rather than aesthetics.

At SLS under global longitudinal bending the following should be verified:

- Stress limitation and web breathing, according to EN-1994, 7.2.
- Deformations: deflections and vibrations, according to EN-1994, 7.3.
- Cracking of concrete, according to EN-1994, 7.4

In this case study we are only analyzing the stress limitation and the cracking of concrete. And we will not carry out a deflection or vibration control, that should be done according to EN-1994, 7.3.

6.5 Stresses control at Serviceability Limit States

6.5.1 CONTROL OF COMPRESSIVE STRESS IN CONCRETE

EN-1994-2, 7.2.2 (1) establishes that the excessive creep and microcraking of concrete shall be avoided by limiting the compressive stress in concrete. EN-1994-2, 7.2.2 (2) refers to EN-1992-1-1 and EN-1992-2, 7.2 for that limitation.

EN-1992-1-1, 7.2 (2) recommends to limit the compressive stress in concrete under the characteristic combination to a value of $k_1 \cdot f_{ck}$ (k_1 is a nationally determined parameter, and the recommended value is 0.60) so as to control the longitudinal cracking of concrete, and also recommends to limit compressive stress in concrete under the quasi-permanent loads to $k_2 \cdot f_{ck}$ (k_2 is a national parameter, and the recommended value is 0.45) in order to admit linear creep assumption.

Fig. 6.14 shows the maximum and minimum normal stresses of the upper concrete slab calculated in two different hypotheses, upper slab cracked or uncracked under the characteristic SLS combination. The results for all cross-sections of the bridge are very far from both compression limits, $0.6 \cdot f_{ck}$=-21 MPa or $0.45 \cdot f_{ck}$=-15.75 MPa.

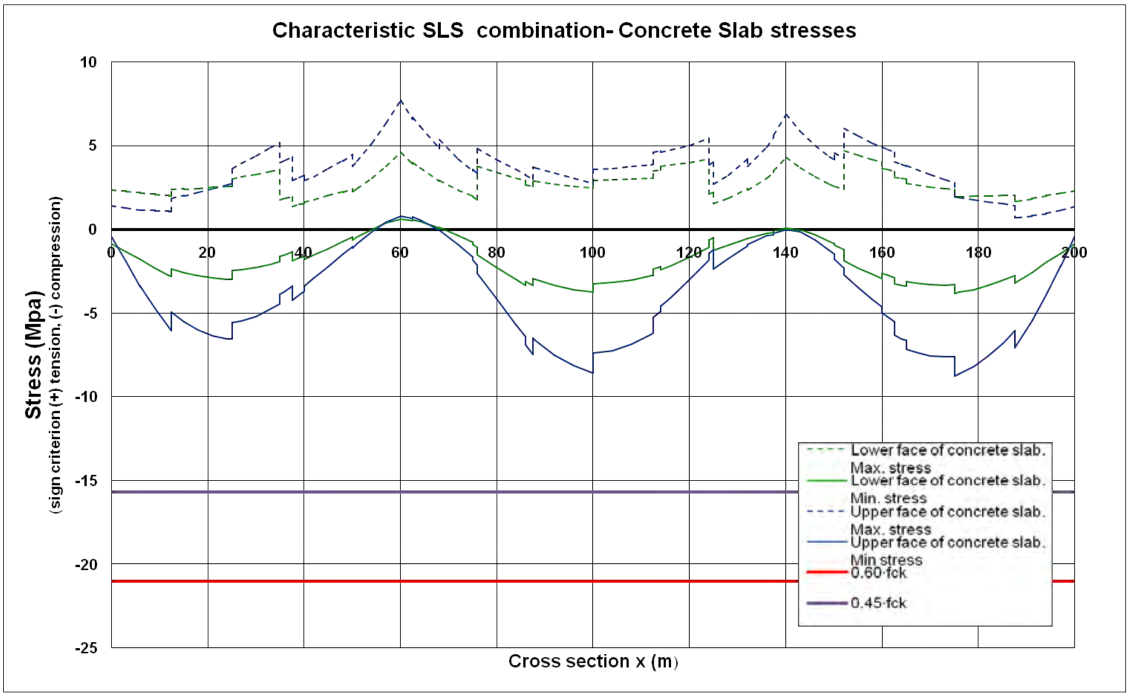

Fig. 6.14 Concrete slab stress under the characteristic SLS combination

6.5.2 CONTROL OF STRESS IN REINFORCEMENT STEEL BARS

Tensile stresses in the reinforcement shall be limited in order to avoid inelastic strain, unacceptable cracking or deformation according to EN-1992-1-1, 7.2(4).

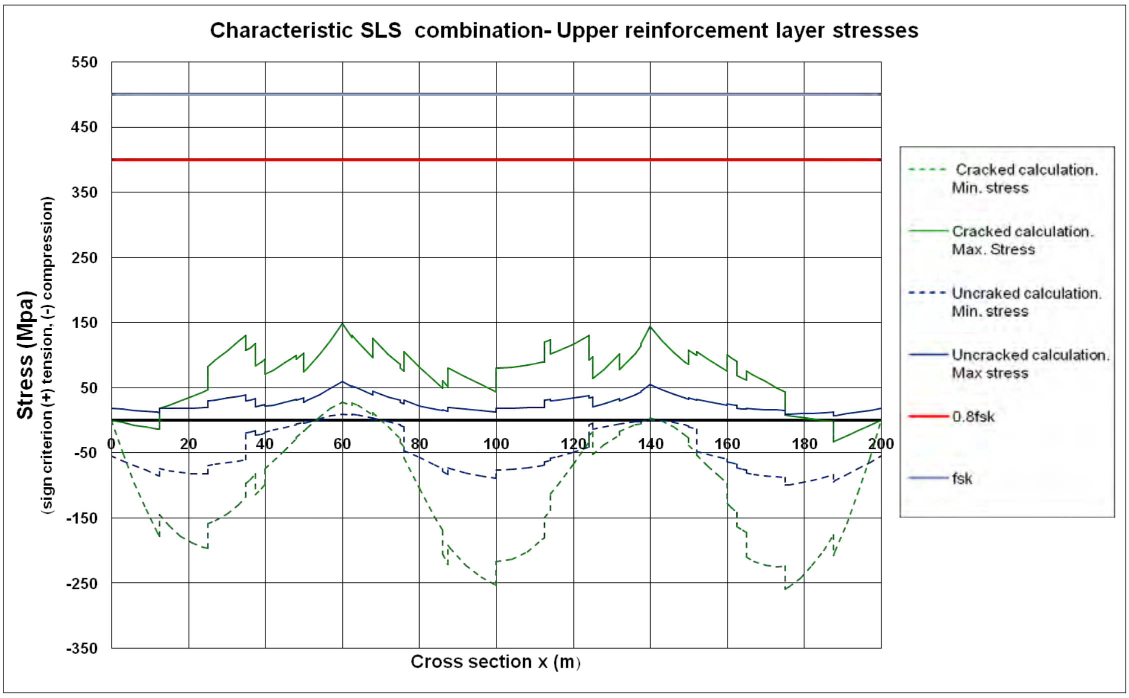

Fig. 6.15 Upper reinforcement layer stress under the characteristic SLS combination

Unacceptable cracking or deformation may be assumed to be avoided if, under the characteristic combination of loads, the tensile stress in the reinforcement does not exceed $k_3 \cdot f_{sk}$, and where the stress is caused by an imposed deformation, the tensile stress should not exceed $k_4 \cdot f_{sk}$. k_3 and k_4 are nationally determined parameters, and the recommended values are k_3= 0.8 and k_4= 1.0).

Fig. 6.15 shows the maximum and minimum normal stresses of the upper reinforcement layer of the slab, calculated in two different hypotheses, upper slab cracked or uncracked under the characteristic SLS combination. The stress results for all cross-sections of the bridge are widely verified for the example, very far from both tensile limits $0.8 \cdot f_{sk}$=400 MPa or $1.0 \cdot f_{sk}$=500 MPa.

Note that the stresses calculated with a contributing concrete strength are not equal to zero at the deck ends because of the shrinkage self-balanced stresses (isostatic or primary effects of shrinkage).

When $M_{c,Ed}$ is negative, the tension stiffening term $\Delta\sigma_s$ should be added to the stress values in Fig. 5.2 calculated without taking the concrete strength into account. This term $\Delta\sigma_s$ is in the order of 100 MPa (see paragraph 6.6.3).

6.5.3 STRESS LIMITATION IN STRUCTURAL STEEL

EN-1994-2, 7.2.2 (5) refers to EN-1993-2, 7.3 for the stress limitation in structural steel under SLS.

For the characteristic SLS combination of actions, considering the effect of shear lag in flanges and the secondary effects caused by deflections (if applicable), the following criteria for the normal and shear stresses in the structural steel should be verified (EN-1993-2, 7.3 equations 7.1, 7.2 and 7.3).

$$\sigma_{Ed,ser} \leq \frac{f_y}{\gamma_{M,ser}}$$

$$\tau_{Ed,ser} \leq \frac{f_y}{\sqrt{3} \cdot \gamma_{M,ser}}$$

$$\sqrt{\sigma^2_{Ed,ser} + 3 \cdot \tau^2_{Ed,ser}} \leq \frac{f_y}{\gamma_{M,ser}}$$

The partial factor $\gamma_{M,ser}$ is a national parameter, and the recommended value is 1.0 according to EN-1993-2, 7.2 (note 2).

Strictly speaking the Von Mises criterion of the third equation only makes sense if it is calculated with concomitant stress values.

For the verification of the stresses control at SLS, the stresses should be considered on the external faces of the steel flanges, and not in the flange midplane (EN-1993-1-1, 6.2.1 (9)).

Figs. 6.16 and 6.17 show the maximum and minimum normal stresses of the upper and lower steel flanges calculated in two different hypotheses, upper slab cracked or uncracked.

The normal stresses for all cross-sections of the bridge are far from the limit of the yield strength, which depends on the steel plate thickness (Figs. 6.16 and 6.17):

$$\sigma_{Ed,ser} \leq \frac{f_y}{\gamma_{M,ser}}$$

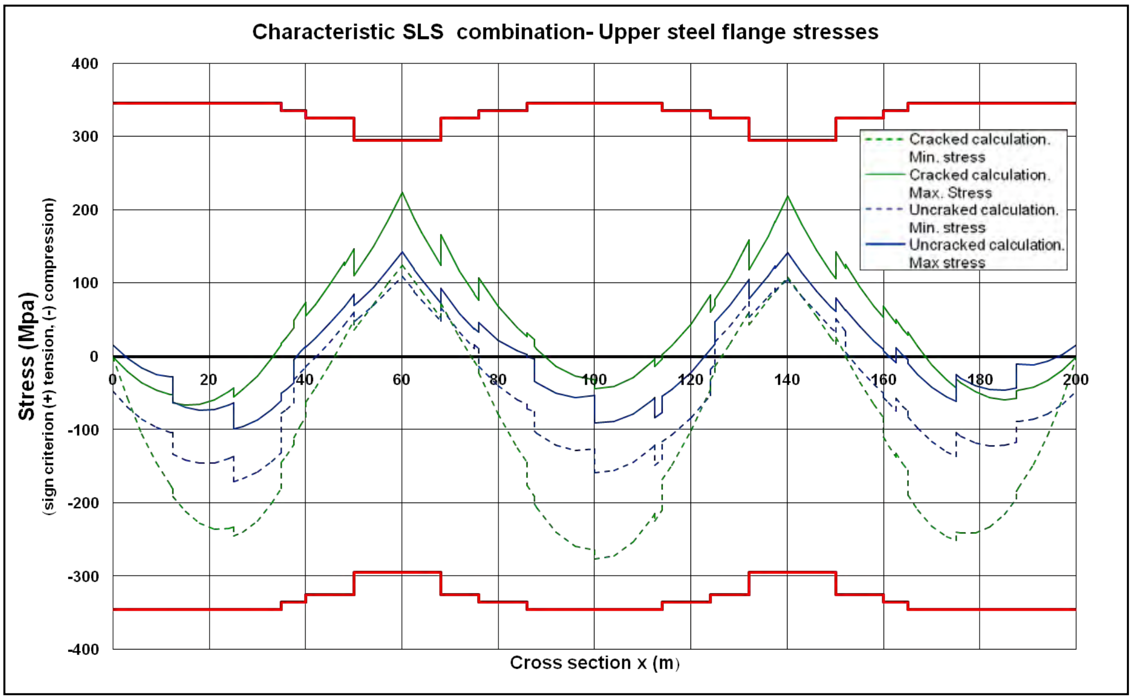

Fig. 6.16 Upper steel flange stress under the characteristic SLS combination

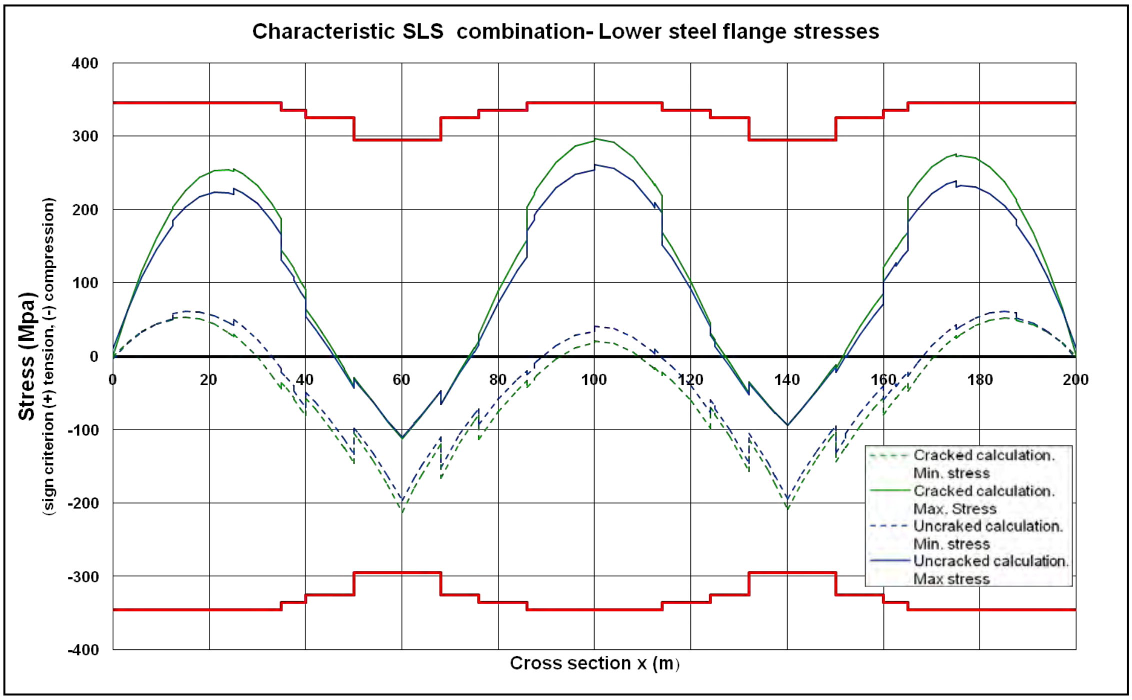

Fig. 6.17 Lower steel flange stress under the characteristic SLS combination

These figures make it clear that the normal stress calculated in the steel flanges without taking the concrete strength into account are logically equal to zero at both deck ends. However this is not true for the stresses calculated by taking the concrete strength into account as the self-balanced stresses from shrinkage (still called isostatic effects or primary effects of shrinkage in EN1994-2) were then taken into account.

Fig. 6.18 shows the maximum and minimum shear stresses in the centroid of the cross section calculated in two different hypotheses, upper slab cracked or uncracked. The shear stress results for all cross-sections of the bridge are very far from the limit:

$$\tau_{Ed,ser} \leq \frac{f_y}{\sqrt{3}\gamma_{M,ser}} = \frac{355}{\sqrt{3} \times 1.0} = 204.96 MPa$$

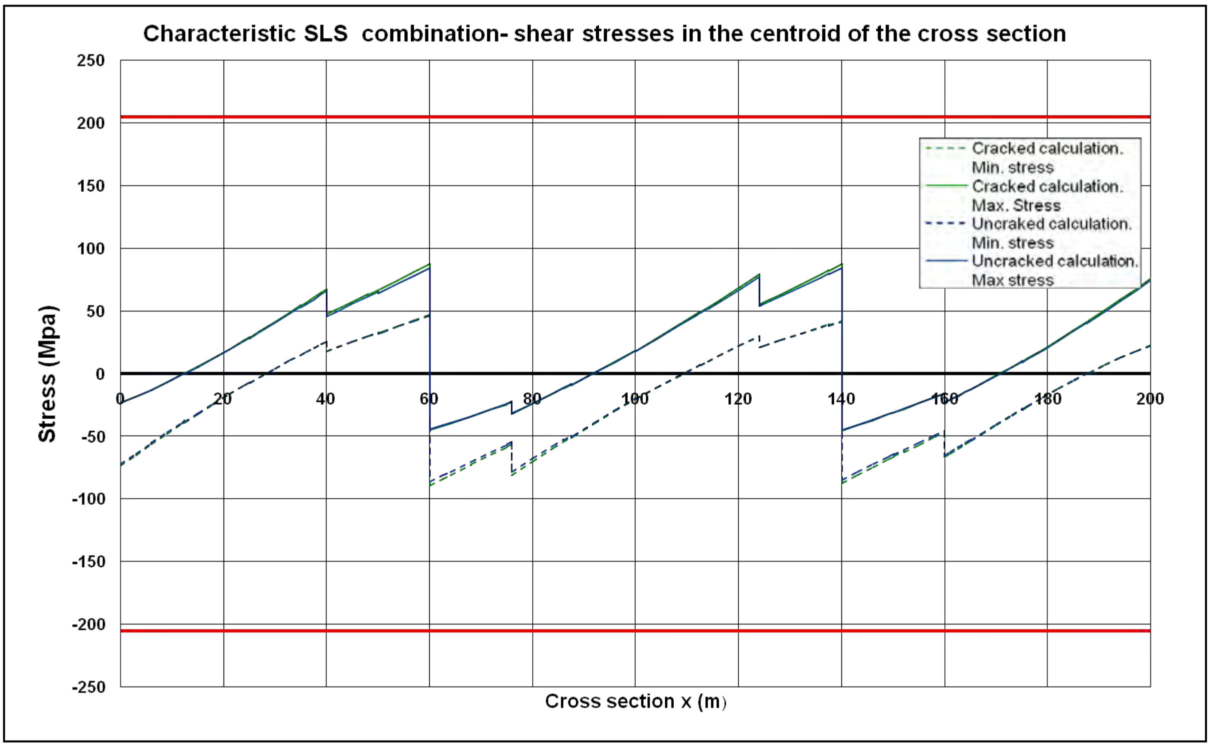

Fig. 6.18 Shear stress in the centre of gravity of the cross-section under the characteristic SLS combination

To be safe without increasing the number of stress calculations (and because this criterion is widely verified for the example, see Figs. 6.19 and 6.20), the Von Mises criterion has been assessed for each steel flange by considering the maximum normal stress in this flange and the maximum shear stress in the web (i.e. non-concomitant stresses and hypotheses on the safe side).

Figs. 6.19 and 6.20 show the maximum and minimum stresses applying the Von Mises safety criterion described in both steel flanges. All cross-sections of the bridge are very far from the limit:

$$\sqrt{\sigma^2_{Ed,ser} + 3\tau^2_{Ed,ser}} \leq \frac{f_y}{\gamma_{M,ser}}$$

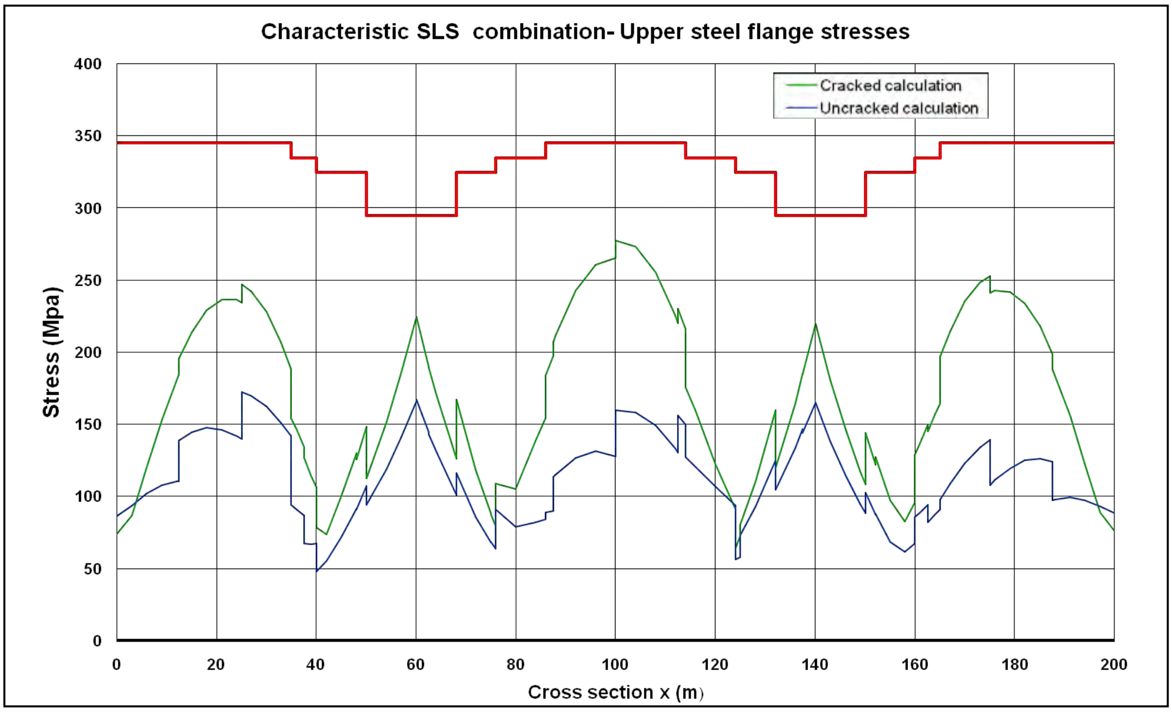

Fig. 6.19 Von Mises criterion in the upper flange under the characteristic SLS combination

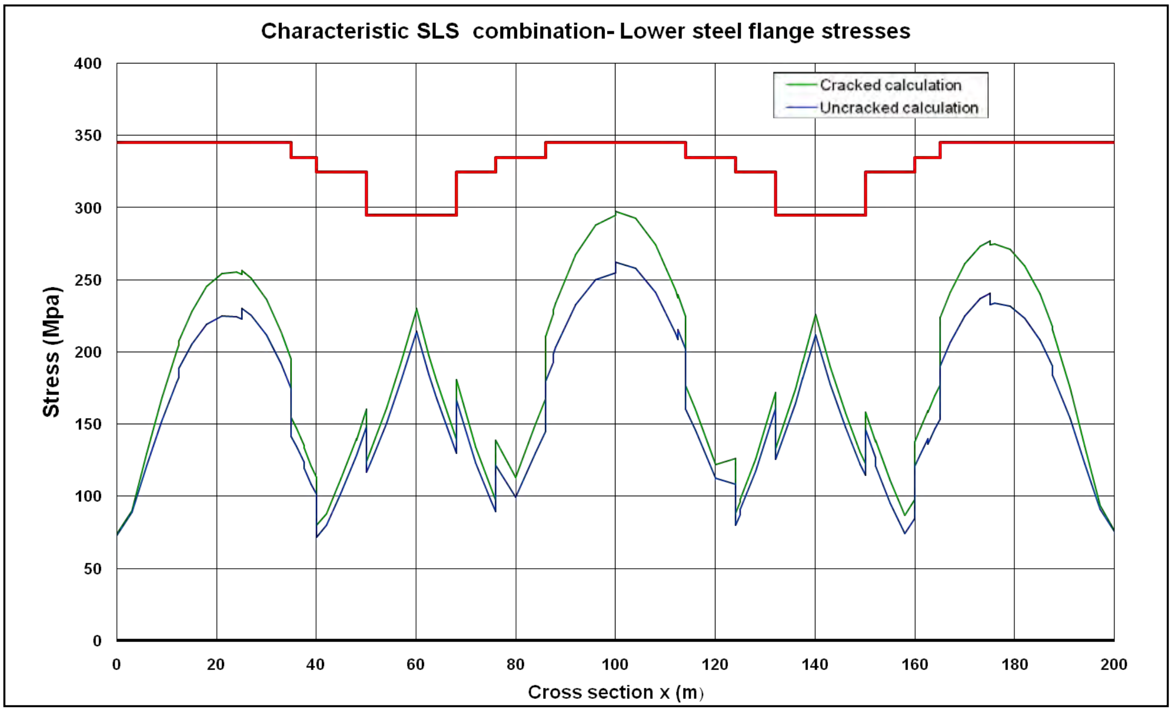

Fig. 6.20 Von Mises criterion in the lower flange under the characteristic SLS combination

6.5.4 ADDITIONAL VERIFICATION OF FATIGUE UNDER A LOW NUMBER OF CYCLES

According to EN-1993-2, 7.3 (2), it is assumed that the nominal stress range in the structural steel framework due to the SLS frequent load combination is limited to:

$$\Delta\sigma_{fre} \le \frac{1.5 f_y}{\gamma_{M,ser}}$$

This criterion is used to ensure that the "frequent" variations remain confined in the strictly linear part (+/- 0.75 f_y) of the structural steel stress-strain relationship. With this, any fatigue problems for a low number of cycles are avoided.

6.5.5 LIMITATION OF WEB BREATHING

Every time a vehicle crosses the bridge, the web gets slightly deformed out of its plane according to the deformed shape of the first buckling mode and then returns to its initial shape. This repeated deformation called web breathing is likely to generate fatigue cracks at the weld joint between web and flange or between web and vertical stiffener.

According to EN-1993-2, 7.4 (2), for webs without longitudinal stiffeners (or for a sub-panel in a stiffened web), the web breathing occurrence can be avoided for road bridges if:

$$\frac{h_w}{t_w} \le 30 + 4.0L \le 300$$

Where L is the span length in m, but not less than 20 m.

For the design example:

- in end-span: h_w/t_w = 151.1 ≤ 30+4·60=270
- in central span: h_w/t_w = 151.1 ≤ 300

Generally speaking this criterion is widely verified for road bridges. Otherwise EN1993-2 defines a more accurate criterion (EN-1993, 7.4 (3)), if EN-1993-2, 7.4 (2) is not satisfied, based on:

- the critical plate buckling stresses of the unstiffened web (or of the sub-panel):

  $\sigma_{cr} = k_\sigma \cdot \sigma_E$ and $\tau_{cr} = k_\tau \cdot \sigma_E$,
- the stresses $\sigma_{x,Ed,ser}$ and $\tau_{x,Ed,ser}$ for frequent SLS combination of actions (calculated at a particular point where fatigue crack initiation could occur):

$$\sqrt{\left(\frac{\sigma_{x,Ed,ser}}{\sigma_{cr}}\right)^2 + \left(\frac{1.1\tau_{x,Ed,ser}}{\tau_{cr}}\right)^2} \le 1.1$$

6.6 Control of cracking for longitudinal global bending

6.6.1 MAXIMUM VALUE OF CRACK WIDTH

The maximum values of the crack width are defined in EN-1992-1-1, 7.31 table 7.1N, depending on the exposure class (EN-1992-1-1, 4 table 4.1).

For the example we assume that the upper reinforcement of the slab, located under the waterproofing layer is XC3 exposure class, and the lower reinforcement of the slab is XC4.

According to EN-1992-1-1, 7.31 table 7.1N, for exposure classes XC3 and XC4 the recommended value of the maximum crack width w_{max} is 0.3 mm under the quasi-permanent load combination.

We will also verify the crack width, limited to w_{max}=0.3 mm, under indirect non-calculated actions (restrained shrinkage), in the tensile zone for the characteristic SLS combination of actions.

6.6.2 CRACKING OF CONCRETE. MINIMUM REINFORCEMENT AREA

The simplified procedure of EN-1994-2, 7.4.2 (1) requires a minimum reinforcement area for the composite beams given by:

$$A_s = k_s k_c k f_{ct,eff} A_{ct} / \sigma_s$$

Where:

$f_{ct,eff}$ is the mean value of the tensile strength of the concrete effective at the time when the cracks may first be expected to occur. $f_{ct,eff}$ may be taken as f_{ctm}=3.2 MPa for a concrete C35/45 (according to EN-1992-1-1 table 3.1).

k is a coefficient which accounts for the effect of non-uniform self balanced stresses. It may be taken equal to 0.80 (EN-1994-2, 7.4.2 (1)).

k_s is a coefficient which accounts for the effect of the reduction of the normal force of the concrete slab due to initial cracking and local slip of the shear connection, which may be taken equal to 0.90 (EN-1994-2, 7.4.2 (1)).

k_c is a coefficient which takes into account the stress distribution within the section immediately prior to cracking, and is given by:

$$k_c = \frac{1}{1 + h_c / \left(2z_0\right)} + 0.3 \leq 1.0$$

h_c is the thickness of the concrete slab, excluding any haunch or ribs. In our case h_c=0.307 m

z_0 is the vertical distance between the centroid of the uncracked concrete flange, and the uncracked composite section, calculated using the modular ratio n_0 for short term loading. In our case, for P-1 cross section, z_0=1.02677-(0.109+0.307/2)= 0.764 m, and for the P1/P2 mid-span cross-section, z_0=0.66854-(0.109+0.307/2)= 0.406 m.

σ_s is the maximum stress permitted in the reinforcement immediately after cracking. This may be taken as its characteristic yield strength f_{sk} (according to EN-1994-2, 7.4.2). In our case f_{sk}=500 MPa.

A_{ct} is the area of the tensile zone, caused by direct loading and primary effect of shrinkage, immediately prior to cracking of the cross section. For simplicity the area of the concrete section within the effective width may be used. In our case A_{ct}=1.95 m^2.

Then:

$k_c = \frac{1}{1 + 0.307 / \left(2 \times 0.764\right)} + 0.3 = 1.13 \leq 1.0$ for the support P-1 cross-section, hence k_c=1.0

$k_c = \frac{1}{1 + 0.307 / \left(2 \times 0.406\right)} + 0.3 = 1.02 \leq 1.0$ for the mid-span P-1-P-2 cross-section, hence k_c=1.0

$A_{s,\min} = 0.9 \times 1.0 \times 0.8 \times 3.2 \times 1.950 \times 10^6 / 500 = 8985.6 mm^2 = 89.85 cm^2$ for half of slab (6 m).

As we have ϕ 20/130 in the upper reinforcement level and ϕ 16/130 in the lower reinforcement level, the reinforcement area is (24.166+15.466) $cm^2/m \cdot 6.0m = 237.79$ $cm^2 >> A_{smin}$, so the minimum reinforcement of the slab is verified.

6.6.3 CONTROL OF CRACKING UNDER DIRECT LOADING

According to EN-1994-2, 7.4.3 (1), when the minimum reinforcement calculated before (according to EN-1994-2, 7.4.2) is provided, the limitation of crack widths may generally be achieved by limiting the maximum bar diameter (according to EN-1994-2 table 7.1), and limiting the maximum bar spacing (according to table 7.2 of EN-1994-2, 7.4.3). Both limits depend on the stress in the reinforcement and the crack width.

Table 6.1 Maximum bar diameter for high bond bars (EN-1994-2, 7.4.3 table 7.2)

Steel Stresses σ_s (N/mm^2)	Maximum bar diameter ϕ^* (mm) for design crack width w_k		
	w_k=0.4 mm	w_k=0.3 mm	w_k=0.2 mm
160	40	32	25
200	32	25	16
240	20	16	12
280	16	12	8
320	12	10	6
360	10	8	5
400	8	6	4
450	6	5	-

The maximum bar diameter ϕ for the minimum reinforcement may be obtained according to EN-1994-2, 7.4.2 (2):

$$\phi = \phi^* \frac{f_{ct,eff}}{f_{ct,0}}$$

Where ϕ^* is obtained of table 7.1 of EN-1994, and $f_{ct,0}$ is a reference strength of 2.9 MPa.

Table 6.2 Maximum bar spacing for high bond bars (EN-1994-2, 7.4.3 table 7.2)

Steel Stresses σ_s (N/mm^2)	Maximum bar spacing (mm) for design crack width w_k		
	w_k=0.4 mm	w_k=0.3 mm	w_k=0.2 mm
160	300	300	200
200	300	250	150
240	250	200	100
280	200	150	50
320	150	100	-
360	100	50	-

The stresses in the reinforcement should be determined taking into account the effect of tension stiffening of concrete between cracks. In EN-1994-2, 7.4.3 (3) there is a simplified procedure for calculating this.

In a composite beam where the concrete slab is assumed to be cracked, stresses in reinforcement increase due to the effect of tension stiffening of concrete between cracks compared with the stresses based on a composite section neglecting concrete.

The direct tensile stress in the reinforcement σ_s due to direct loading may be calculated according to EN-1994-2, 7.4.3 (3)

$$\sigma_s = \sigma_{s,0} + \Delta\sigma_s$$

With $\Delta\sigma_s = \dfrac{0.4 f_{ctm}}{\alpha_{st}\rho_s}$ and $\alpha_{st} = \dfrac{AI}{A_a I_a}$

Where:

- $\sigma_{s,0}$ is the stress in the reinforcement caused by the internal forces acting on the composite section, calculated neglecting concrete in tension.
- f_{ctm} is the mean tensile strength of the concrete. For a concrete C35/45 (according to EN-1992-1-1 table 3.1) f_{ctm}=3.2 MPa.
- ρ_s is the reinforcement ratio, given by $\rho_s = \dfrac{A_s}{A_{ct}}$
- A_{ct} is the area of the tensile zone. For simplicity the area of the concrete section within the effective width may be used. In our case A_{ct}=1.95 m^2.
- A_s is the area of all layers of longitudinal reinforcement within the effective concrete area.
- A, I are area and second moment of area, respectively, of the effective composite section neglecting concrete in tension.
- A_a, I_a are area and second moment of area, respectively, of the structural steel section.

Although there could be another section of the bridge with higher tensile stresses in the reinforcement, due to the sequence of the concreting phase, we will check for the application example only two cross sections, over the support P-1, which normally would be the worst section, and mid span P-1/P-2.

At the P-1 cross-section: A_s=237.79 cm^2 (ϕ 20/130 + ϕ 16/130 in 6 m), hence $\rho_s = \dfrac{237.79\times10^{-4}}{1.95} = 0.01219$, and the mid-span P-1/P-2 cross-section A_s=185.59 cm^2 (ϕ 16/130 + ϕ 16/130 in 6 m), hence $\rho_s = \dfrac{185.59\times10^{-4}}{1.95} = 0.00952$.

The value of α_{st} at the P-1cross-section is $\alpha_{st} = \dfrac{0.3543\times0.5832}{0.3305\times0.5076} = 1.232$, while in the mid-span P-1/P-2 cross-section $\alpha_{st} = \dfrac{0.1555\times0.2456}{0.1369\times0.1969} = 1.416$.

Then, the effect of tension-stiffening at the P-1 cross-section is:

$$\Delta\sigma_s = \frac{0.4\times3.2}{1.232\times0.01219} = 85.23 MPa$$

Meanwhile in the mid span P-1/P-2: $\Delta\sigma_s = \dfrac{0.4\times3.2}{1.416\times0.0} = 94.95MPa$

As the tensile stresses in the reinforcement caused by the internal forces acting on the composite section, calculated neglecting concrete in tension are:

- Support P-1 cross section: $\sigma_{s,0}$ =65.94 MPa
- Mid span P-1/P-2 cross section: $\sigma_{s,0}$ =27.45 MPa

Then the direct tensile stresses in reinforcement σ_s due to direct loading (according to EN-1994-2, 7.4.3) are:

- Support P-1 cross section: $\sigma_s = \sigma_{s,0} + \Delta\sigma_s$ =65.94+85.23=151.17 MPa
- Mid span P-1/P-2 cross section: $\sigma_s = \sigma_{s,0} + \Delta\sigma_s$ =27.45+94.95=122.4 MPa

As both values are below 160 MPa, according to table 6.2, the maximum bar spacing for the design crack width w_k=0.3mm is 300 mm. As we have 130 mm, the maximum bar spacing is verified.

According to table 6.1, the maximum bar diameter ϕ^* for the minimum reinforcement should be 32 mm, and

$$\phi = 32\frac{3.2}{2.9} = 35.31mm$$

As the example verifies the minimum reinforcement established by EN-1994-2, 7.4.2 (1), the actual maximum diameter used in the longitudinal steel reinforcement is ϕ20, lower than the limit established by EN-1994-2, 7.4.2 (2), and the bar spacing also verifies the limits established by EN-1994-2, 7.4.2 (3), then the crack width is controlled.

6.6.4 CONTROL OF CRACKING UNDER INDIRECT LOADING

It has to be verified that the crack widths remain below 0.3 mm using the indirect method in the tensile zones of the slab for characteristic SLS combination of actions. This method assumes that the stress in the reinforcement is known. But that is not true under the effect of shrinkages (drying, endogenous and thermal shrinkage). The following conventional calculation is then suggested:

From the expression of the minimum reinforcement area for the composite beams given by EN-1994-2, 7.4.2 (1) $A_s = k_s k_c k f_{ct,eff} A_{ct} / \sigma_s$ we can get:

$$\sigma_s = k_s k_c k f_{ct,eff} A_{ct} / A_s$$

Let´s consider that this is the stress in the reinforcement due to shrinkage at the cracking instant.

In our case, for the P-1 cross-section: As=237.79 cm^2 (ϕ20/130 + ϕ16/130 in 6 m), and the mid span P-1/P-2 cross section As=185.59 cm^2.

This gives:

- Support P-1 cross section: σ_s=0.9x1.0x0.8x3.2x1.95 / (237.79x10^{-4})=188.94 MPa
- Mid-span P-1/P-2 cross section: σ_s=0.9x1.0x0.8x3.2x1.95 / (185.59x10^{-4})=242.08 MPa

High bond bars with diameter ϕ= 20 mm have been chosen in the upper reinforcement layer of the slab at the support cross-section, and ϕ= 16 mm at the mid-span P-1/P-2 cross section. This gives:

- Support P-1 cross-section: ϕ^*= ϕ·2.9/3.2=18.125 mm

- Mid-span P-1/P-2 cross-section: $\phi^{*}=\phi\cdot 2.9/3.2=14.5$ mm

The maximum reinforcement stress is obtained by linear interpolation in Table 7.1 in EN1994-2:

- Support P-1 cross-section: 230.18 MPa >188.94 MPa
- Mid-span P-1/P-2 cross-section: 255.00 MPa>242.08 MPa

Hence both sections are verified.

6.7 Shear connection at steel-concrete interface

6.7.1 RESISTANCE OF HEADED STUDS

The design shear resistance of a headed stud (Fig. 6.22) (P_{Rd}) automatically welded in accordance with EN-14555 is defined in EN-1994-2, 6.6.3:

$$P_{Rd} = \min(P^{(1)}{}_{Rd}; P^{(2)}{}_{Rd})$$

$P^{(1)}{}_{Rd}$ is the design resistance when the failure is due to the shear of the steel shank toe of the stud:

$$P^{(1)}{}_{Rd} = \frac{0.8 f_u \dfrac{\pi d^2}{4}}{\gamma_v}$$

$P^{(2)}{}_{Rd}$ is the design resistance when the failure is due to the concrete crushing around the shank of the stud:

$$P^{(2)}{}_{Rd} = \frac{0.29 \alpha d^2 \sqrt{f_{ck} E_{cm}}}{\gamma_v}$$

With:

$$\alpha = 0.2\left(\frac{h_{sc}}{d}+1\right) \text{ for } 3 \le \frac{h_{sc}}{d} \le 4$$

$$\alpha = 1.0 \text{ for } \frac{h_{sc}}{d} > 4$$

Where:

γ_v is the partial factor. The recommended value is γ_V=1.25.

d is the diameter of the shank of the headed stud (16≤d≤25mm).

f_u is the specified ultimate tensile strength of the material of the stud (f_u≤500MPa).

f_{ck} is the characteristic cylinder compressive strength of the concrete. In our case f_{ck}=35 MPa.

E_{cm} is the secant modulus of elasticity of concrete (EN-1992-1-1, 3.1.2 table 3.1). In our case $E_{cm}=22000(f_{cm}/10)^{0.3}=34077.14$ MPa. ($f_{cm}=f_{ck}+8$ MPa)

h_{sc} is the overall nominal height of the stud.

In our case, if we consider headed studs of steel S-235-J2G3 of diameter d=22 mm, height h_{sc}=200 mm, and f_u=450 MPa, then:

$$P^{(1)}_{Rd} = \frac{0.8 \times 450 \times \frac{\pi \times 22^2}{4}}{1.25} = 0.1095 \times 10^6 \text{ N=0.1095 MN}$$

$$\frac{h_{sc}}{d} = \frac{200}{22} = 9.09 >> 4\,,\ \alpha = 1.0 \text{ and } P^{(2)}_{Rd} = \frac{0.29 \times 1 \cdot 22^2 \times \sqrt{35 \times 34077.14}}{1.25} = 0.1226 \text{ MN}$$

Then: $P_{Rd} = 0.1095$ MN. Each row of 4 headed studs (Fig. 6.21) resist at ULS: $4 \cdot P_{Rd} = 0.438$ MN

For Serviceability State Limit, EN-1994, 7.2.2 (6) refers to 6.8.1 (3). Under the characteristic combination of actions the maximum longitudinal shear force per connector should not exceed $k_s \cdot P_{Rd}$ (the recommended value for k_s=0.75).

Then: $k_s \cdot P_{Rd} = 0.75 \times 0.1095$ MN=0.0766 MN. Each row of 4 headed studs (Fig. 6.21) resist at SLS: $4 \cdot k_s \cdot P_{Rd} = 0.3064$ MN

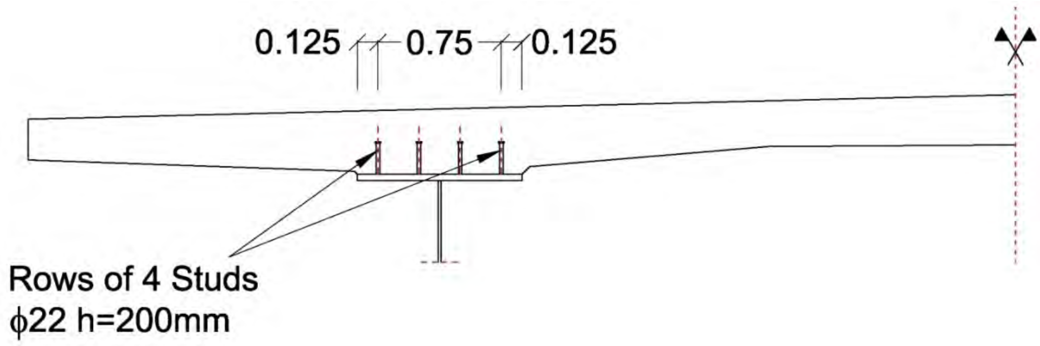

Fig. 6.21 Detail of headed studs connection

6.7.2 DETAILING OF SHEAR CONNECTION

The following construction detailing applies for in-situ poured concrete slabs (EN-1994-2, 6.6.5). When the slab is precast, these provisions may be reviewed paying particular attention to the various instability problems (buckling in the composite upper flange between two groups of shear connectors, for example) and to the lack of uniformity of the longitudinal shear flow at the steel-concrete interface (EN-1994-2, 6.6.5.5 (4))

Maximum longitudinal spacing between rows of connectors

According to EN-1994-2, 6.6.5.5 (3), to ensure a composite behaviour of the main girder, the maximum longitudinal center to center spacing (s) between two successive rows of connectors is limited to: $s_{max} \leq$ min (800 mm ; 4 h_c), with h_c the concrete slab thickness.

When verifying the mid-span P1/P2 cross-section (see paragraph 6.1.2), it was considered that the upper structural steel flange in compression was a Class 1 element as it was connected to the concrete slab.

However if we consider the upper flange non-connected to the upper concrete slab, according to EN-1993-1-1 table 5.2 sheet 2 of 3, c/t_f = ((1000-18)/2)/40=12.275 and that would result a Class 4 flange as $c/t_f = 12.275 > 14\cdot = 14 \times \sqrt{235/345} = 11.55$

In order to classify a compressed upper flange connected to the slab as a Class 1 or 2 because of the restraint from shear connectors, the headed studs rows should be sufficiently close to each other to prevent buckling between two successive rows (EN-1994-2, 6.6.5.5(2)). This gives an additional criterion in s_{max} :

$s_{max} \le 22 t_f \sqrt{235/fy}$ if the concrete slab is solid and there is contact over the full length.

$s_{max} \le 15 t_f \sqrt{235/fy}$ if the concrete slab is not in contact over the full length (e.g. slab with transverse ribs). This is not our case.

Where t_f is the thickness of the upper flange, and f_y the yield strength of the steel flange.

Table 6.3 summarizes the results of applying both conditions to our case.

Table 6.3 Maximum longitudinal spacing for rows of studs

Upper Steel flange t_f (mm)	**f_y (N/mm^2)**	**s_{max}**	**e_D**
40	345	726	297
55	335	800	414
80	325	800	*
120	295	800	*

* Only applies for flanges in compression (not in tension)

This criterion is supplemented by EN-1994-2, 6.6.5.5(2) defining a maximum distance between the longitudinal row of shear connectors closest to the free edge of the upper flange in compression – to which they are welded – and the free edge itself (Fig. 6.22):

$$e_D \le 9 \times t_f \sqrt{235/fy}$$

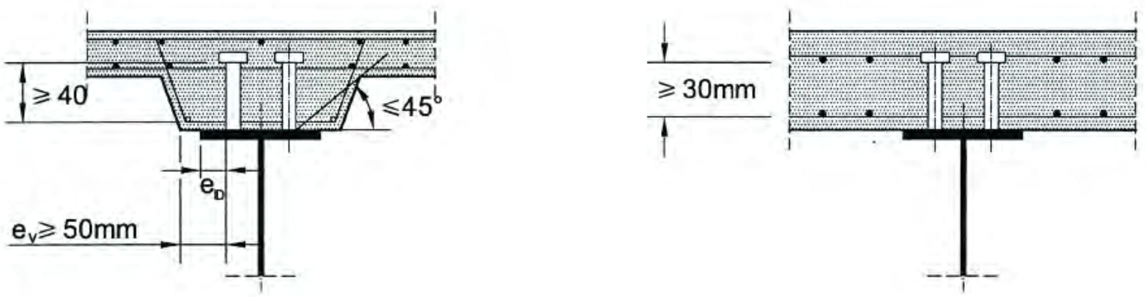

Fig. 6.22 Detailing

Minimum distance between the edge of a connector and the edge of a plate

According to EN-1994-2, 6-6-5-6 (2), the distance e_D between the edge of a headed stud and the edge of a steel plate must not be less than 25 mm, in order to ensure the correct stud welding.

In this example (Fig. 6.21), $e_D = \frac{b_f - b_0}{2} - \frac{d}{2} = \frac{1000 - 750}{2} - \frac{22}{2} = 114 > 25$

Minimum dimensions of the headed studs

According to EN-1994-2 6.6.5.7 (1) and (2) the height of a stud should not be less than *3·d*, where d is the diameter of the shank, and the head of the stud should have a diameter not less than *1.5·d*, and a depth of at least *0.4·d* (Fig. 6.23).

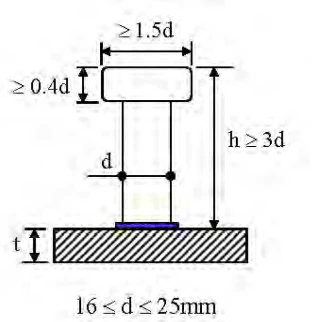

Fig. 6.23 Minimum dimensions of a headed stud

As we have studs of *d*=22 mm, the head should have a diameter over 33 mm, and a depth of at least 8.8 mm. With a total height of the studs of 200 mm, we are far from the limit of 3·*d*=66 mm.

EN-1994-2 also establishes a condition between the diameter of the connector and the thickness of the steel plate (EN-1994-2, 6.6.5.7 (3)). For studs welded to steel plates in tension subjected to fatigue loading, the diameter of the stud should be:

$$d \leq 1.5 \cdot t_f$$

This is widely satisfied in the example, with t_{fmin}=55mm in the tensile area, and *d*=22mm.

This limitation also applies to steel webs. This verification allows the use of the detail category $\Delta\tau_c$ = 90 MPa.

Clause 6.6.5.7 (5) establishes that the limit for other elements than plates in tension or webs is $d \leq 2.5 \cdot t_f$

Minimum spacing between rows of connectors

According to EN-1994-2 6.6.5.6 (4) the longitudinal spacing of studs in the direction of the shear force should be not less than 5*d*=110 mm in our case, while the spacing in the transverse direction to the shear force should be not less than 2.5*d* in solid slabs, or 4*d* in other cases. In our example 2.5*d*=55 mm. Both limits are widely fulfilled in the example, with s_{trans}=250 mm

Criteria related to the stud anchorage in the slab

Where a concrete haunch is used between the upper structural steel flange and the soffit of the concrete slab, the sides of the haunch should lie outside a line drawn 45º from the outside edge of the connector (Fig. 6.22) (EN-1994-2, 6.6.5.4 (1)).

Clause 6.6.5.4 (2) establishes that the nominal concrete lateral cover from the side of the haunch to the connector should not be less than 50 mm, and the clear distance between the lower face of the stud head and the lower reinforcement layer should be not less than 40 mm, according to clause

6.6.5.4 (2). This value could be reduced to 30 mm if no concrete haunch is used (EN-1994-2 6.6.5.1 (1)) (see Fig. 6.22).

Figs. 6.24 and 6.25 show a general view and a detail of the connection with headed studs of the upper flange of a composite bridge, and Fig. 6.26 shows the connection of the lower flange of the main steel girders in a double composite cross-section.


Figs. 6.24 & 6.25 View and detail of an upper flange connection

Fig. 6.26 View of the lower flange connection of a steel girder

6.7.3 CONNECTION DESIGN FOR THE CHARACTERISTIC SLS COMBINATION OF ACTIONS

When the structure behaviour remains elastic in a given cross-section, each load case from the global longitudinal bending analysis produces a longitudinal shear force per unit length $v_{L,k}$ at the interface between the concrete slab and the steel main girder. For a girder with uniform moment of area (S) subjected to a continuous bending moment, this shear force per unit length is easily deduced from the cross-section properties and the internal forces and moments the girder is subjected to:

$$v_{L,k} = \frac{S_c V_k}{I}$$

Where:

$v_{L,k}$ is the longitudinal shear force per unit length at the interface concrete-steel

S_c is the moment of area of the concrete slab with respect to the centre of gravity of the composite cross-section

I is the second moment of area of the composite cross-section

V_k is the shear force for the considered load case and coming from the elastic global cracked analysis

According to EN-1994-2, 6.6.2.1 (2), to calculate normal stresses, when the composite cross-section is ultimately (characteristic SLS combination of actions in this paragraph) subjected to a negative bending moment $M_{c,Ed}$, the concrete is taken as cracked and does not contribute to the cross-section strength. But to calculate the shear force per unit length at the interface, even if $M_{c,Ed}$ is negative, the characteristic cross-section properties S_c and I are calculated by taking the concrete strength into account (uncracked composite behaviour of the cross-section).

The final shear force per unit length is obtained by adding algebraically the contributions of each single load case and considering the construction phases. As for the normal stresses calculated with an uncracked composite behaviour of the cross-section, the modular ratio used in S_c and I is the same as the one used to calculate the corresponding shear force contribution for each single load case.

For SLS combination of actions, the structure behaviour remains entirely elastic and the longitudinal global bending calculation is performed as an envelope. Thus the value of the shear force per unit length is determined in each cross-section at abscissa x by:

$$v_{L,k}(x) = \max\left[\left|v_{\min,k}(x)\right|;\left|v_{\max,k}(x)\right|\right]$$

Fig. 6.27 shows the variations in this longitudinal shear force per unit length for the characteristic SLS combination of actions, for the case of the example.

In each cross-section of the deck there should be enough studs to resist all the shear force per unit length.

The following should be therefore verified at all abscissa x:

$$v_{L,k}(x) \le \frac{N_i}{L_i} \cdot (k_s \cdot \mathrm{P}_{Rd}) \text{ , with } k_s \cdot P_{RD} = 4 \cdot k_s \cdot P_{RD,\text{ of 1 stud}}$$

Where:

$v_{L,k}$ is the shear force per unit length in the connection under the characteristic SLS combination

N_i is the number of rows of 4 headed studs ϕ22mm and h=200 mm located at the length L_i

L_i is the length of a segment with constant row spacing

$k_s \cdot P_{Rd} = 4 \cdot k_s \cdot P_{Rd,\text{ of 1 stud}} = 0.3064\ MN$ is the SLS resistance of a row of 4 headed studs, calculated in 7.1

For the example we have divided the total length of the bridge into segments delimited by the following abscissa x in (m), corresponding with nodes of the design model:

0.0	6.0	12.5	25.0	35.0	42.0	50.0	62.5
80.0	87.5	100.0	108.0	112.5	120.0	132.0	140.0
150.0	162.5	170.0	176.0	187.5	194.0	200.0	

For example, for the segment [50.0 m ; 62.5 m] around the support P1, the shear force per unit length obtained in absolute value for characteristic SLS combination of actions is as follows (in MN/m):

Table 6.4 Shear force per unit length at SLS at segment 50-62.5 m

x (m)	50^+	54^-	54^+	60^-	60^+	62.5^-
$\boldsymbol{v_{L,k}}$ **(MN/m)**	0.842	0.900	0.900	0.989	0.943	0.906

The maximum SLS shear force per unit length to be considered is therefore 0.989 MN/m, which is guaranteed providing the stud rows are placed at the maximum spacing of (4 studs per row):

$$\frac{(4 \cdot k_s \cdot P_{Rd})}{\max\left(v_{L,k}(x)\right)} = \frac{0.3064 \text{ MN}}{0.989 \text{ MN/m}} = 0.31 \text{ m}$$; on a safe side 0.30 m.

Fig. 6.27 illustrates this elastic design of the connection for characteristic SLS combination of actions. The curve representing the shear force per unit length that the shear connectors are able to take up thus encompasses fully the curve of the SLS design shear force per unit length.

The corresponding values of row spacing, obtained for the design of the connection in SLS are summarized in paragraph 6.7.5 of this chapter. Note that we have considered regular spacing jumps from 50 to 50 mm.

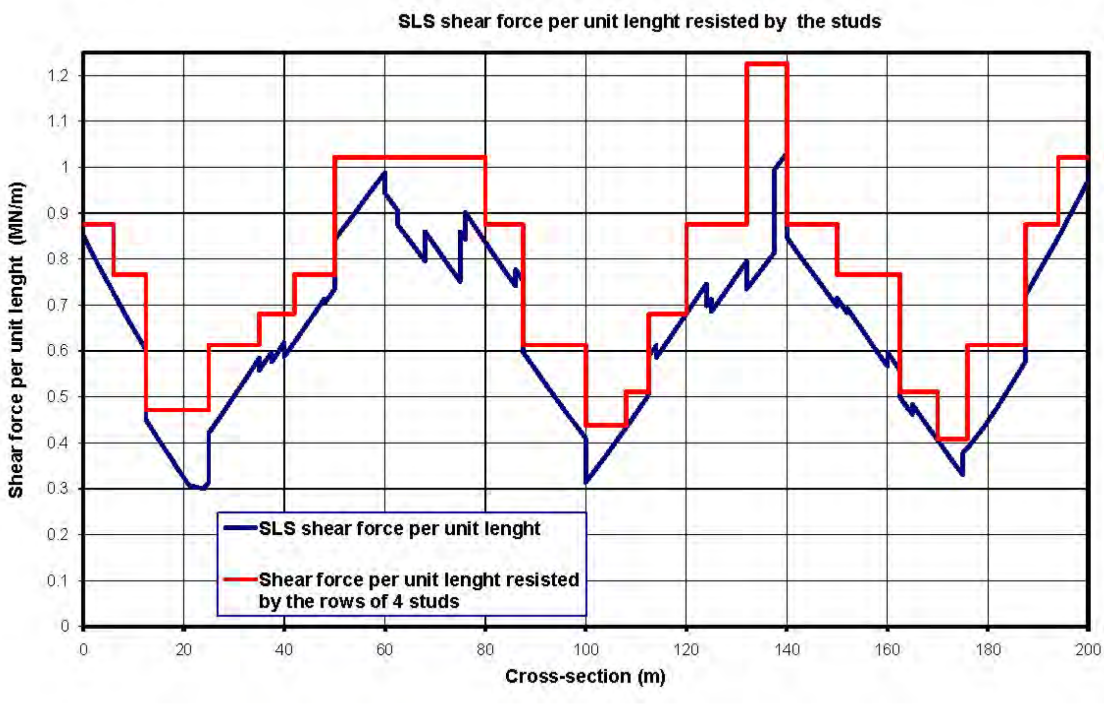

Fig. 6.27 SLS shear force per unit length resisted by the headed studs

6.7.4 CONNECTION DESIGN FOR THE ULS COMBINATION OF ACTIONS OTHER THAN FATIGUE

6.7.4.1 Elastic design

Whatever the behaviour of the bridge at ULS – elastic in all cross-sections or elasto-plastic in some cross-sections – the design of the connection at ULS starts by an elastic calculation of the shear force per unit length at the interface steel-concrete, by elastic analysis with the cross-sections properties of the uncracked section taking into account the effects of construction (EN-1994, 6.6.2.2 (4)), following the same procedure as made for SLS in the previous paragraph.

In each cross-section, the shear force per unit length at ULS is therefore given by:

$$v_{L,Ed}(x) = \max\left[\left|v_{\min,Ed}(x)\right|;\left|v_{\max,Ed}(x)\right|\right]$$

With:

$$v_{L,Ed} = \frac{S_c V_{Ed}}{I}$$

Where:

$v_{L,Ed}$ is the design longitudinal shear force per unit length at the concrete-steel interface.

S_c is the moment of area of the concrete slab with respect to the centre of gravity of the composite cross-section.

I is the second moment of area of the composite cross-section.

V_{Ed} is the design shear force for the considered load case and coming from the elastic global cracked analysis considering the constructive procedure.

Fig. 6.28 shows the variations in this design longitudinal shear force per unit length for the ULS combination of actions, for the case of the example.

According to EN-1994-2, 6.6.1.2 (1) the number of shear connectors (headed studs) per unit length, constant per segment, should verify the following two criteria:

- locally in each segment *"i"*, the shear force per unit length should not exceed by more than 10% what the number of shear connectors per unit length can resist:

  $$v_{L,Ed}(x) \le 1.1 \cdot \frac{N_i}{L_i} \cdot P_{RD}\text{, with } P_{RD} = 4 \cdot P_{RD,\ of\ 1\ stud}$$

  Where:

  N_i is the number of rows of 4 headed studs ϕ22mm and h=200 mm located at the length L_i

  L_i is the length of a segment with constant row spacing

  $P_{Rd}=4 \cdot P_{Rd,\ of\ 1\ stud} = 0.438\ MN$ is the ULS resistance of a row of 4 headed studs, calculated in 7.1.

- over every segment length (L_i), the number of shear connectors should be sufficient so that the total design shear force does not exceed the total design shear resistance:

$$\int_{x_i}^{x_{i+1}} v_{L,Ed}(x)\, dx \leq N_i(P_{RD}) \text{ , with } P_{RD} = 4 \cdot P_{RD,\text{ of } 1\, stud}$$

Where x_i *and* x_{i+1} designates the abscissa at the border of the segment L_i.

For the design of the connection at ULS we have considered the same segment division as used for the SLS verification.

In the example, for the segment [50.0 m ; 62.5 m] around the support P1, the design shear force per unit length obtained in absolute value for ULS combination of actions is as follows (in MN/m):

Table 6.5 Design shear force per unit length at ULS at segment 50-62.5 m

x (m)	50^+	54^-	54^+	60^-	60^+	62.5^-
$v_{L,Ed}$ **(MN/m)**	1.124	1.203	1.203	1.323	1.264	1.213

The maximum ULS design shear force per unit length to be resisted is therefore 1.323 MN/m, which is guaranteed providing the stud rows are placed at the maximum spacing of (4 studs per row):

$$\frac{1.10 \times (4 \cdot \mathrm{P}_{Rd,\ 1\ stud})}{\max\left(v_{L,kEd}(x)\right)} = \frac{1.1 \times 0.438 \text{ MN}}{1.323 \text{ MN/m}} = 0.365 \text{ m}$$

And the second condition:

$$\int_{x_i}^{x_{i+1}} v_{L,Ed}(x)\, dx = 15.407 MN \text{ (in 12.5 m)=1.232 MN/m} \leq \frac{(4 \cdot \mathrm{P}_{Rd,\ 1\ stud})}{s}$$

Then $s \geq (4 \cdot P_{Rd,\ of\ 1\ stud})/1.232$= 0.438/1.232=0.355 m, then on the safe side the spacing for this segment would be s=0.35 m.

Fig. 6.28 illustrates the elastic design of the connection for the Ultimate Limit State (ULS) combination of actions.

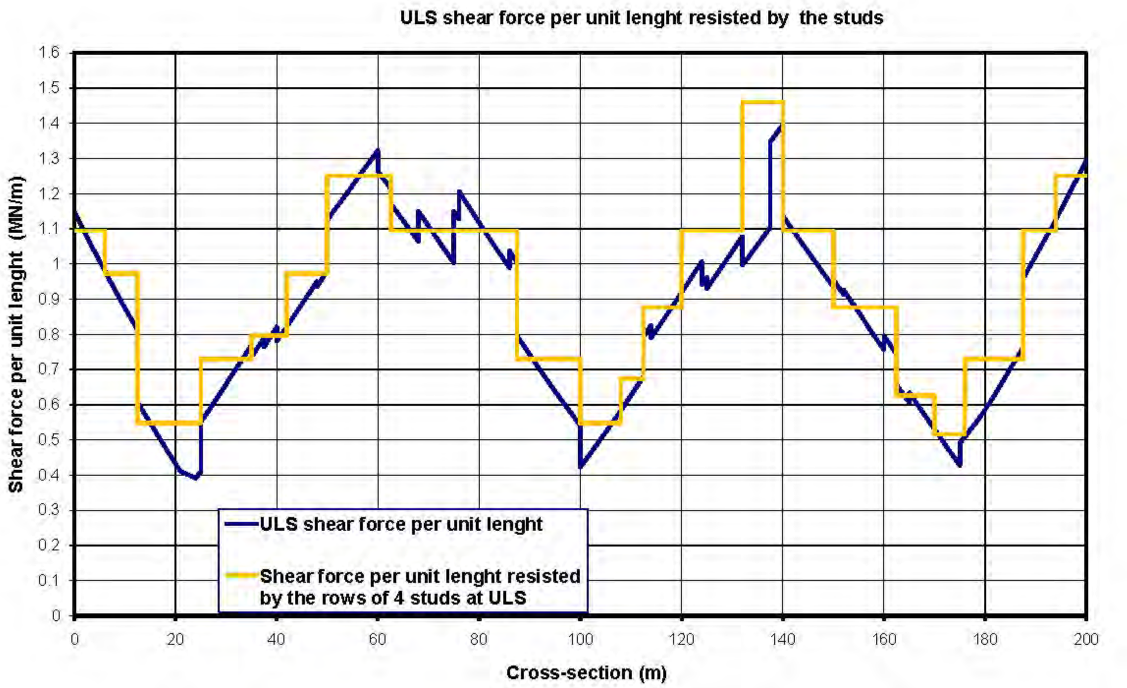

Fig. 6.28 ULS shear force per unit length resisted by the headed studs

6.7.4.2 Design with plastic zones in sagging bending areas

If, a cross-section with a positive bending moment at ULS has partially yielded, the previous elastic calculation, made for the ULS combination of actions, should be supplemented (EN-1994-2, 6.6.2.2 (1)).

As far as the structure behaviour is no longer elastic, the relationship between the shear force per unit length and the global internal forces and moments is no longer linear. Therefore the previous elastic calculation becomes inaccurate. In a plastic zone, the shear connection is normally heavily loaded and a significant bending moment redistribution occurs between close cross-sections.

In our case, although the mid-span cross-sections are Class 1 sections, no yielding occurs, as we can see on Fig. 6.1, with a medium tensile value for the lower flange of 342.9MPa < f_y=345MPa. There is therefore no need to perform the more complex calculations established by EN-1994-2 in clauses 6.6.2.2 (2) and (3).

6.7.5 SYNOPSIS OF THE DESIGN EXAMPLE

Paragraphs 6.7.3 and 6.7.4 summarize, respectively, the connection design at SLS and ULS. Fig. 6.29 shows the results of the spacing of rows of 4 headed stud connectors resulting from the design at SLS (red solid line), the design at ULS (orange solid line), and the results of applying the maximum spacing requirements (green solid line) defined in paragraph 6.7.1, according to EN-1994-2.

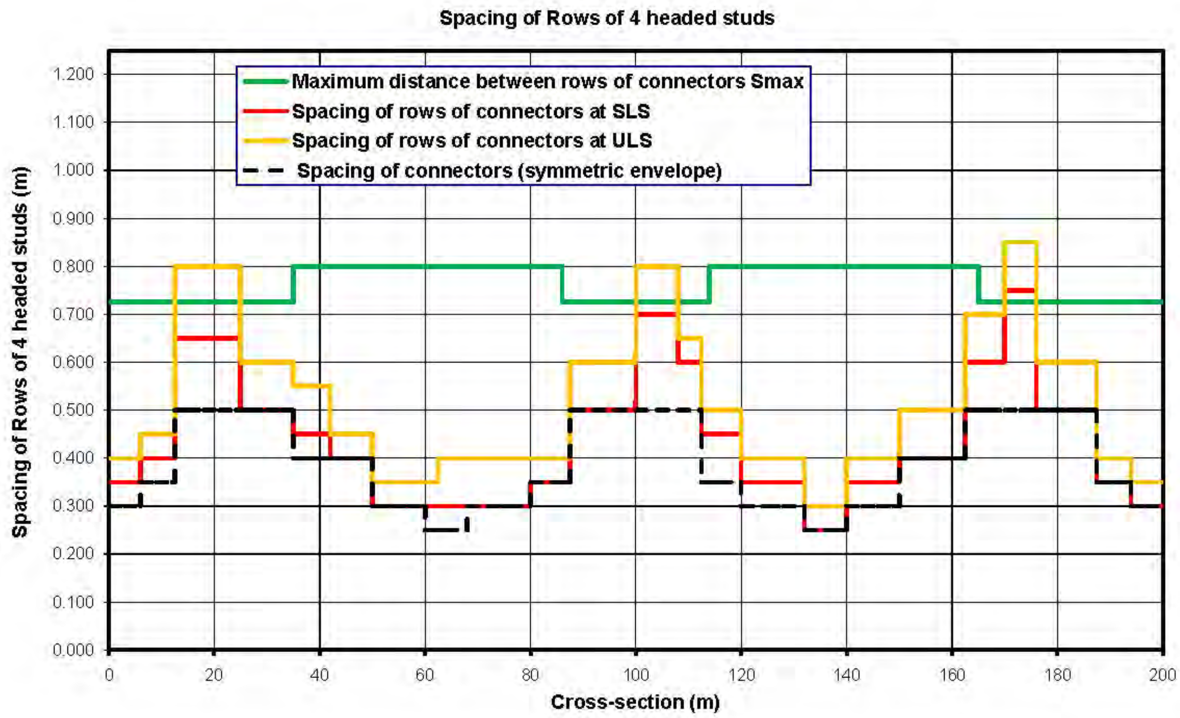

Fig. 6.29 Envelope of spacing of rows of 4 connectors after connection dimensioning

As described before, we have used an engineering criterion of dimensioning the spacing of rows of connectors, with 50 mm steps. This figure also shows the final envelope (in black dotted line) resulting from the three mentioned conditions, and with the provision of symmetrical spacing design of the connection in the total length of the bridge. Although that could not be theoretically necessary, constructively thinking it is absolutely convenient.

Note that, in general, the SLS criteria nearly always govern the design over the ULS requirements, except for the sections around the mid-span. In these zones, the spacing just necessary to resist the SLS shear flow becomes too large to avoid buckling in the steel flange between two successive stud rows. And then the governing criterion becomes the construction detailing.

6.7.6 DESIGN OF THE SHEAR CONNECTION FOR THE FATIGUE ULS COMBINATION OF ACTIONS

In this paragraph we summarize the fatigue verification that has to be performed to confirm the design of the connection already performed in previous paragraphs under SLS and ULS combination of actions.

Once the connection is designed, and decided the final spacing of rows of connectors, fatigue ULS of the connectors has to be verified according to EN-1994-2, section 6.8.

The fatigue load model FLM3 induces the following stress ranges:

- o $\Delta\tau$, shear stress range in the stud shank, calculated at the level of its weld on the upper structural steel flange.

  Unlike normal stress range, the shear stresses at the steel-concrete interface are calculated using the uncracked cross-section mechanical properties. The shear stress for the basic combination of non-cyclic loads (EN1992-1-1, 6.8.3) has therefore no influence. $\Delta\tau$ is thus deduced from variations in the shear force per unit length under the FLM3 crossing only – noted $\Delta v_{L,FLM3}$ – by taking account of its transverse location on the pavement and using the short term modular ratio n_0. $\Delta\tau$ also depends on the local shear connector density and the nominal value of the stud shank area:

$$\Delta\tau = \frac{\Delta v_{L,FLM3}}{\left(\frac{\pi d^2}{4}\right)\frac{N_i}{L_i}}$$

Where:

N_i is the number of rows of 4 headed studs ϕ 22mm and h=200 mm located at the length *Li*.

L_i is the length of a segment with constant row spacing.

d is the diameter of the shank of the headed stud.

$\Delta v_{L,FLM3}$ is the variations in the shear force per unit length under the FLM3 crossing.

- $\Delta\sigma_p$, normal stress range in the upper steel flange to which the studs are welded.

6.7.6.1 Equivalent constant amplitude stress range

For verification of stud shear connectors based on nominal stress ranges, the equivalent constant range of shear stress $\Delta\tau_{E,2}$ for two million cycles is given by (EN-1994-2, 6.8.6.2(1)):

$$\Delta\tau_{E,2} = \lambda_v \cdot \Delta\tau$$

Where:

$\Delta\tau$ is the range of shear stress due to fatigue loading, related to the cross-sectional area of the shank of the stud $\pi d^2/4$ with d the diameter of the shank.

λ_v is the damage equivalent factor depending on the spectra and the slope m of the fatigue curve.

For bridges, the damage equivalent factor λ_v for headed studs in shear should be determined from $\lambda_v = \lambda_{v1} \cdot \lambda_{v2} \cdot \lambda_{v3} \cdot \lambda_{v4}$ (EN-1994-2, 6.8.6.2 (3))

Factors λ_{v2} to λ_{v4} should be determined in accordance with EN-1993-2, 9,5,2 (3) to (6) but using exponents 8 and 1/8 instead of 5 and 1/5, to allow for the relevant slope m=8 of the fatigue strength curve for headed studs given in EN-1994-2, 6.8.3 (3).

- λ_{v1} is the factor for damage effect of traffic. According to EN-1994-2, 6.8.6.2 (4) λ_{v1}=1.55 for road bridges up to 100 m span.
- λ_{v2} is the factor for the traffic volume

$$\lambda_{v2} = \frac{Q_{m1}}{Q_0}\left(\frac{N_{obs}}{N_0}\right)^{1/8}$$

Where:

$Q_{m1} = \left[\frac{\sum n_i Q_i^8}{\sum n_i}\right]^{1/8}$ (EN-1993-2, 9.5.2 (3)) is the average gross weight (kN) of the lorries in the slow lane.

Q_0=480KN

N_0=0.5x10^6

N_{obs} is the total number of lorries per year in the slow lane. In this example we have N_{obs}=0.5x10^6, equivalent to a road or motorway with medium rates of lorries (EN-1991-2, table 4.5 (n))

Q_i is the gross weight in kN of the lorry *i* in the slow lane.

n_i is the number of lorries of gross weight Q_i in the slow lane.

Table 6.6 Traffic assumption for obtaining λ_{v2}

Lorry	Q (kN)	Long. distance
1	200	20%
2	310	5%
3	490	50%
4	390	15%
5	450	10%

If we substitute table 6.6 values into the previous equations, then we obtain:

Q_{m1}=457.37 kN

$$\lambda_{v2} = \frac{457.37}{480} = 0.952$$

- o λ_{v3} is the factor for the design life of the bridge. For 100 years of design life, then λ_{v3}=1.0 according to EN-1993-2, 9.5.2 (5)
- o λ_{v4} takes into account the effects of the heavy traffic on the other additional slow lane defined in the example. In the case of a single slow lane, λ_{v4}=1.0.

In the present case, the factor depends on the transverse influence of each slow lane on the internal forces and moments in the main girders:

$$\lambda_{v4} = \left[1 + \frac{N_2}{N_1}\left(\frac{\eta_2 Q_{m2}}{\eta_1 Q_{m1}}\right)^8\right]^{1/8}$$

$$\eta = \frac{1}{2} - \frac{e}{b}$$

With

e is the eccentricity of the FLM3 load with respect to the bridge deck axis (in the example +/- 1.75 m);

b is the distance between the main girders (in the example 7.0 m).

$$\eta_1 = \frac{1}{2} + \frac{1.75}{7.0} = 0.75 \text{ and } \eta_2 = \frac{1}{2} - \frac{1.75}{7.0} = 0.25$$

The factor η_l represents the maximum influence of the transverse location of the traffic slow lanes on the fatigue-verified main girder. $N_1=N_2$ (same number of heavy vehicles in each slow lane) and $Q_{m1}=Q_{m2}$ (same type of lorry in each slow lane) will be considered for the example.

This gives finally λ_{v4}=1.0.

Then λ_v=1.55·0.952·1.0·1.0=1.477

For the upper steel plate, a stress range $\Delta\sigma_E$ is defined according to EN-1994-2, 6.8.6.1 (2):

$$\Delta\sigma_{\mathrm{E}} = \lambda\phi\left|\sigma_{\max,f} - \sigma_{\min,f}\right|$$

Where:

$\sigma_{max,f}$ and $\sigma_{min,f}$ are the maximum and minimum stresses due to the maximum and minimum internal bending moments resulting from the combination of actions defined in EN-1992-1-1, 6.8.3 (3):

$$\left(\sum_{j\geq 1} G_{k,j} \text{"+"} P \text{"+"} \psi_{1,1} Q_{k,1} \text{"+"} \sum_{i>1} \psi_{2,i} Q_{k,i}\right) \text{"+"} Q_{fat}$$

λ is the damage equivalent factor, calculated according to EN-1993-2, 9.5.2., for road bridges, with the relevant slope of the fatigue strength curve m=5.

ϕ is a damage equivalent impact factor. For road bridges ϕ = 1.0 (EN-1994-2, 6.8.6.1 (7)), however ϕ is increased when crossing an expansion joint, according to EN-1991-2. 4.6.1(6), ϕ =1.3[1-D/26]≥1.0, where D (in m) is the distance between the detail verified for fatigue and the expansion joint (with D≤6m).

6.7.6.2 Fatigue verifications

For stud connectors welded to a steel flange that is always in compression under the relevant combination of actions (see paragraph 7.6.1), the fatigue assessment should be made by checking the criterion, which corresponds to a crack propagation in the stud shank:

$$\gamma_{Ff}\Delta\tau_{E-2} \leq \Delta\tau_c / \gamma_{Mf,s}$$

Where:

$\Delta\tau_{E,2}$ is the equivalent constant range of shear stress for two millions cycles

$\Delta\tau_{E,2} = \lambda_v \cdot \Delta\tau$ (see paragraph 7.6.1)

$\Delta\tau_c$ is the reference value of fatigue strength at 2 million cycles. $\Delta\tau_c$=90 MPa

γ_{Ff} is the fatigue partial factor. According to EN-1993-2, 9.3 the recommended value is γ_{Ff}=1.0

$\gamma_{Mf,s}$ is the partial factor for verification of headed studs in bridges. According to EN-1994-2, 2.4.1.2 (6), the recommended value is $\gamma_{Mf,s}$=1.0.

Meanwhile, where the maximum stress in the steel flange to which studs connectors are welded is tensile under the relevant combination, the interaction at any cross-section between shear stress range $\Delta\tau_E$ in the weld of the stud connector and the normal stress range $\Delta\sigma_E$ in the steel flange should be verified according to EN-1994-2, 6.8.7.2 (2):

$$\frac{\gamma_{Ff}\Delta\sigma_{E,2}}{\Delta\sigma_c / \gamma_{Mf}} \leq 1.0 \ ; \ \frac{\gamma_{Ff}\Delta\tau_{E,2}}{\Delta\tau_c / \gamma_{Mf,s}} \leq 1.0 \ \text{ and } \ \frac{\gamma_{Ff}\Delta\sigma_{E,2}}{\Delta\sigma_c / \gamma_{Mf}} + \frac{\gamma_{Ff}\Delta\tau_{E,2}}{\Delta\tau_c / \gamma_{Mf,s}} \leq 1.3$$

Where:

$\Delta\sigma_E$ is the stress range in the flange connected (see paragraph 7.6.1)

$\Delta\sigma_c$ is the reference value of fatigue strength at 2 million cycles. $\Delta\sigma_c$=80 MPa

γ_{Mf} is the partial factor defined by EN-1993-1-9 table 3.1. For safe life assessment method with high consequences of the upper steel flange failure of the bridge, γ_{Mf}=1.35.

In general, once the connection at the steel-concrete interface is designed under the SLS and ULS combination of actions, and the final spacing of connectors is decided fulfilling the maximum spacing limits established by EN-1994-2 (see paragraphs 6.7.2 to 6.7.5), the fatigue ULS verification does not influence the design of the connection.

Figure 6.30 shows the verification of the connection under the fatigue ULS, for the case of the example, and Figure 6.31 shows the spacing of the rows of 4 studs under the fatigue ULS.

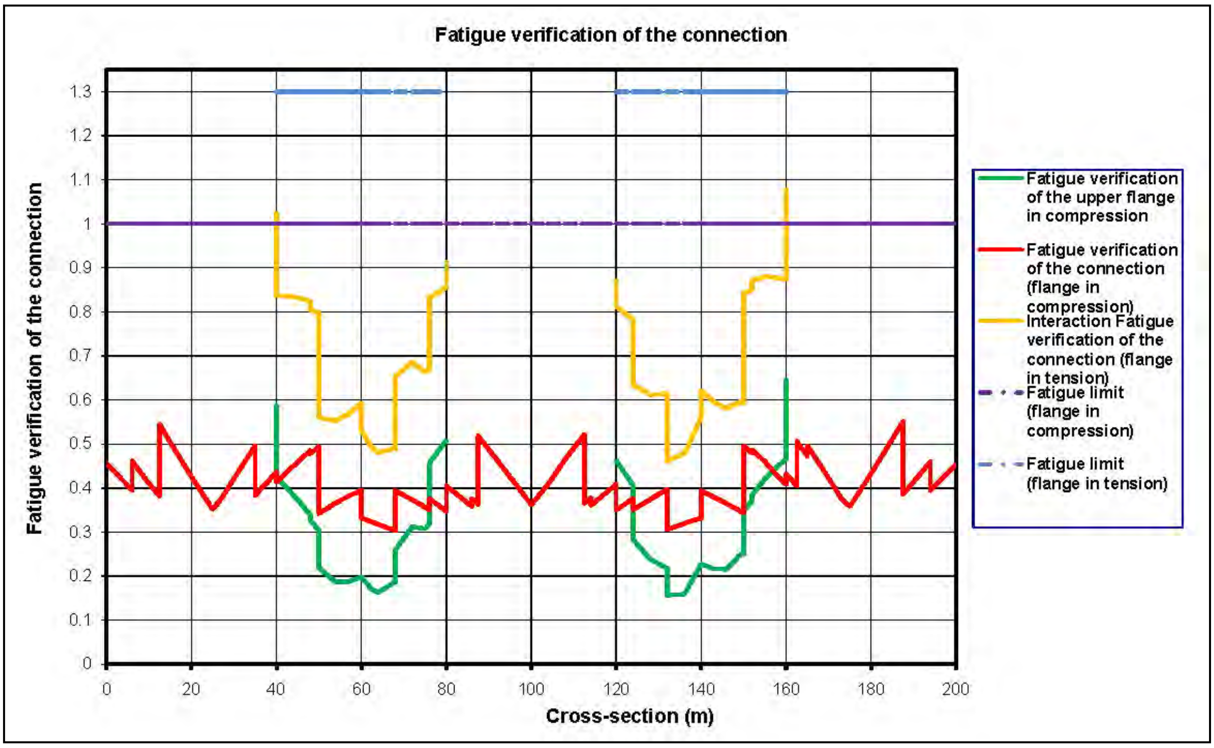

Fig. 6.30 Fatigue verification of the connection

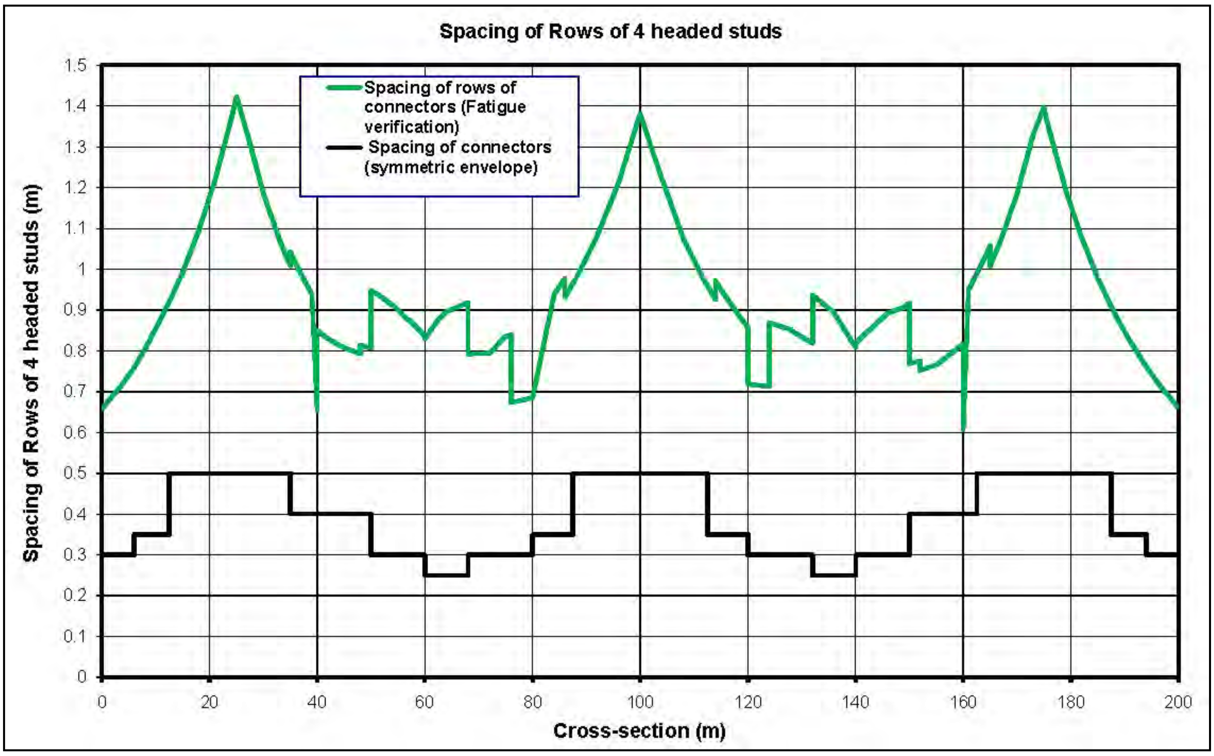

Fig. 6.31 Spacing of the rows of connectors under the fatigue ULS

6.7.7 INFLUENCE OF SHRINKAGE AND THERMAL ACTION ON THE CONNECTION DESIGN AT BOTH DECK ENDS

The shear force per unit length at the steel/concrete interface, used in the previous calculations, only takes account of hyperstatic (or secondary) effects of shrinkage and thermal actions. It is therefore necessary to also verify, according to EN-1994-2 6.6.2.4 (1), that sufficient shear connectors have been put in place at both free deck ends, to anchor the shear force per unit length coming from the isostatic (or primary) effects of shrinkage and thermal actions.

The first step is to calculate – in the cross-section at a distance L_v from the free deck end (anchorage length) – the normal stresses due to the isostatic effects of the shrinkage (envelope of short-term and long-term calculations) and thermal actions.

Integrating these stresses over the slab area gives the longitudinal shear force at the steel/concrete interface for the two considered load cases.

The second step is to determine the maximum longitudinal spacing between stud rows over the length L_v which is necessary to resist the corresponding shear force per unit length. The calculation is performed for ULS combination of actions only. In this case, EN1994-2, 6.6.2.4 (3) considers that the studs are ductile enough for the shear force per unit length $v_{L,Ed}$ to be assumed constant over the anchorage length L_v. This length is taken as equal to b_{eff}, which is the effective slab width in the global analysis at mid-end span (6 m for this example).

All calculations performed for the design example, a maximum longitudinal shear force of 2.15 MN is obtained at the steel/concrete interface under shrinkage action (obtained with the long-term calculation) and 1.14 MN under thermal actions.

This therefore gives $V_{L,Ed}$ = 1.0x2.15 + 1.5x1.14 = 3.86 MN for ULS combination of actions.

Notice that according to EN-1992-1-1, 2.4.2.1 (1) the recommended partial factor for shrinkage action is γ_{SH}=1.0.

The design value of the shear flow $v_{L,Ed}$ (at ULS) and then the maximum spacing s_{max} over the anchorage length L_v= b_{eff} between the stud rows are as follows:

$$v_{L,Ed} = \frac{V_{L,Ed}}{b_{eff}} = 0.643 \text{ MN/m} \quad \text{(rectangular shear stress block)}$$

$$s_{\max} = \frac{4P_{Rd,\,1\,stud}}{v_{L,Ed}} = \frac{0.438}{0.643} = 0.681 \text{ m}$$

This spacing is significantly higher than the one already obtained through previous verifications (see Fig. 7.9). As it is generally the case, the anchorage of the shrinkage and thermal actions at the free deck ends does not govern the connection design.

Notes:

- To simplify the design example, the favourable effects of the permanent loads are not taken into account (self-weight and non-structural bridge equipments). Anyway they cause a shear flow which is in the opposite direction to the shear flow caused by shrinkage and thermal actions. So the suggested calculation is on the safe side.

  Note that it is not always true. For instance, for a cross-girder in a cantilever outside the main steel girder and connected to the concrete slab, the shear flow coming from external load cases should be added to the shear flow coming from shrinkage and thermal actions. Finally the shear flow for ULS combination of these actions should be anchored at the free end of the cross-girder.

- EN1994-2, 6.6.2.4(3) suggests that the same verification could be performed by using the shear flow for SLS combination of actions and a triangular variation between the end cross-section and the one at the distance L_v. However, this will never govern the connection design and it is not explicitly required by section 7 of EN1994-2 dealing with the SLS justifications.

References

EN-1992-1-1: Eurocode 2: Design of concrete structures. Part 1-1: General rules and rules for buildings.

EN-1992-2: Eurocode 2: Design of concrete structures. Part 2: Concrete bridges- Design and detailing rules.

EN-1993-1-1: Eurocode 3: Design of steel structures. Part 1-1: General rules and rules for buildings.

EN-1993-1-5: Eurocode 3: Design of steel structures. Part 1-5: Platted steel structures.

EN-1993-2: Eurocode 3: Design of steel structures. Part 2: Steel bridges.

EN-1994-1-1: Eurocode 4: Design of composite steel and concrete structures. Part 1-1: General rules and rules for buildings.

EN-1994-2: Eurocode 4: Design of composite steel and concrete structures. Part 2: General rules and rules for bridges.

L.Davaine, F. Imberty, J. Raoul. 2007. "*Guidance book. Eurocodes 3 and 4. Application to steel-concrete composite road bridges".*Sétra.

C.R. Hendy and R.P. Johnson. 2006. *"Designers' Guide to EN-1994-2. Eurocode 4: Design of composite steel and concrete structures. Part 2: General rules and rules for bridges"*. Great Britain: Thomas Telford.